1

Foundations of Confocal Scanned Imaging in Light Microscopy

Shinya Inoué

Seldom has the introduction of a new instrument generated as instant an excitement among biologists as the laser-scanning confocal microscope. With the new microscope, one can slice incredibly clean, thin optical sections out of thick fluorescent specimens; view specimens in planes tilted to, and even running parallel to, the line of sight; penetrate deep into light-scattering tissues; gain impressive three-dimensional (3D) views at very high resolution; obtain differential interference or phase-contrast images in exact register with confocal fluorescence images; and improve the precision of microphotometry.

While the instrument that engendered such excitement became commercially available first in 1987, the optical and electronic theory and the technology that led to this sudden emergence had been brewing for several decades. The development of this microscope stems from several roots, including light microscopy, confocal imaging, video and scanning microscopy, and coherent or laser-illuminated optics (see historic overview in Table 1.1). In this chapter, I will first discuss some basic principles relating to lateral and axial resolution as well as depth of field in light microscopy, highlight some history that lays a foundation to the development of laser-scanning confocal microscopy, and end with some general remarks regarding the new microscopes, including a disk-scanning confocal system.

LIGHT MICROSCOPY

Lateral Resolution[1]

The foundations of modern light microscopy were established a century ago by Ernst Abbe (1873, 1884). He demonstrated how the diffraction of light by the specimen, and by the objective lens, determined image resolution; defined the conditions needed to design a lens whose resolution was diffraction limited (rather than limited by chromatic and spherical aberrations); and established the role of the objective and condenser numerical apertures (NA) on image resolution (Eq. 1). Thus,

$$d_{\min} = \frac{1.22\lambda_o}{\mathrm{NA}_{obj} + \mathrm{NA}_{cond}} \qquad \textbf{(1)}$$

where $d_{\min}$ is the minimum spacing *in a periodic grating* that can just be resolved. $d_{\min}$ is expressed as lateral distance in the specimen space; λ_o is the wavelength of light in vacuum; and NA_{obj} and NA_{cond} are the numerical apertures of the objective and condenser lenses, respectively. The NA is the product of the sine of the half-angle (α) of the cone of light either acceptable by the objective lens or emerging from the condenser lens and the refractive indexes (η) of the imbibing medium between the specimen and the objective or condenser lens, respectively.

Equation 1 demonstrates that, in addition to the wavelength and the NA of the objective lens, the condenser NA also affects image resolution in the microscope. For objects that are illuminated fully coherently (a condition that pertains when NA_{cond} approaches 0, namely when the condenser iris is closed down to a pinhole), the minimum resolvable lateral spacing **increases** (i.e., **the resolution decreases**) by a factor of 2 compared to the case when the condenser iris is opened so that $NA_{cond} = NA_{obj}$. As the condenser iris is opened and NA_{cond} becomes larger, the illumination becomes progressively less coherent and resolution increases. [Note, however, that laser beams tend to illuminate objects coherently even when the condenser iris is not closed down (see Chapter 5, *this volume*).]

Equation 1 describes the relation between NA and resolution for line-grating objects. A complementary method of defining the limit of resolution uses point objects instead of line gratings. The image, in focus, of an infinitely small luminous object point is itself not infinitely small, but is a circular Airy diffraction image with a central bright disk and progressively weaker concentric dark and bright rings. The radius r_{Airy} of the first dark ring around the central disk of the Airy diffraction image depends on λ and the NA of the objective:

$$r_{Airy} = 0.61\frac{\lambda_o}{\mathrm{NA}_{obj}} \qquad \textbf{(2)}$$

where r_{Airy} is expressed as distance in the specimen plane.

When there exist two points of light separated by a small distance d in the specimen plane, their diffraction images lie side by side in the image plane. The images of two equally bright spots are said to be resolved if d is larger or equal to the radius of the Airy disk. This is the Rayleigh criterion, and it relies on the assumption that the two point sources radiate incoherently. If the two point sources emit light coherently, their amplitude rather than

[1] For extensive discussions on modern microscope lens design and aberrations and a more rigorous treatment of the optical principles and applications of light microscopy than is appropriate for this revised chapter, refer to complementary chapters in *Handbook of Optics* (e.g., Inoué and Oldenbourg, 1994) and in *Video Microscopy*, *2nd edition* (Inoué and Spring, 1997).

Shinya Inoué • Marine Biological Laboratory, Woods Hole, Massachusetts 02543

TABLE 1.1. Historic Overview[a]

Confocal Microscopy	Microscopy	Video (Microscopy)
	Abbe (1873, 1884)[a,c]	Nipkow (1884)
	Berek (1927)[d]	
		Zworykin (1934)
	Zernicke (1935)[a,c]	
	Gabor (1948)[a]	
	Hopkins (1951)[a]	Flory (1951)
		Young and Roberts (1951)
		Flying spot[c]
	Linfoot and Wolf (1953)	
	3D diffraction by annul. apert.[a,d]	
	Tolardo di Francia (1955)	
	Limited field[b]	
	Nomarski (1955)[a]	
	Linfoot and Wolf (1956)	Montgomery *et al*. (1956)
	3D diffraction pattern[a,d]	Flying spot UV[c]
	Ingelstam (1956)	
	Resolution and info. theory[a]	
Minsky Patent (1957)		
Insight[a,b,c,d]		
Stage scanning[f]		
	Kubota and Inoué (1959)[a,c]	
	Smith and Osterberg (1961)[a]	
		Freed and Engle (1962)
		Flying spot[c]
	Harris (1964)[a,b]	
	Ellis (1966)	
	Holomicrography[a]	
Petráň *et al.* (1968)		
Tandem scanning[d,g]		
Davidovits and Egger (1971)		
Laser illumination		
Lens scanning[d]		
	Hellwarth and Christensen (1974)	
	Second harmonic generation[c,d]	
	Hoffman and Gross (1975)	
	Modulation contrast[c]	
Sheppard and Choudhury (1977)		
Theory[a,b,d]		
Sheppard *et al.* (1978)	Ellis (1978)	
Stage scanning[c,d,e,f]	Single sideband edge enhancement microscopy[c,d]	
Cremer and Cremer (1978)		
Auto-focus stage scanning[d]		
"4-π-point illumination"[a,b,d]		
Brakenhoff *et al.* (1979)		Castleman (1979)
Specimen scan[a,b,d,e]		Digital image processing[a,c,e]
Koester (1980)	Quate (1980)	
Scanning mirror[d]	Acoustic microscopy[a,c]	
		Inoué (1981)[a,c]
		Allen *et al.* (1981a,b)[a,c]
		Fuchs *et al.* (1982)[f]
		Agard and Sedat (1983)[a,c,d]
Cox and Sheppard (1983)		
Digital recording[d,e]		
Åslund *et al.* (1983)		
2-mirror laser scanning[d]		
Hamilton *et al.* (1984)		
Differential phase[c,d]		
Wilson and Sheppard (1984)		
Extended depth of field[c,d,e,f]		
Boyde (1985a)	Ellis (1985)	Sher and Barry (1985)[f]
Nipkow type[d,e]	Light scrambler[d]	Fay *et al.* (1985)[a,c,d]
Carlsson *et al.* (1985)		
Laser scan, Stacks of confocal images[d,e]		
Wijnaendts van Resandt *et al.* (1985)		
xz-view[d,e]		

TABLE 1.1. (*Continued*)

Confocal Microscopy	Microscopy	Video (Microscopy)
Suzuki-Horikawa (1986)	Cox and Sheppard (1986)	Inoué (1986)
Video-rate laser scan[g]		Overview, How to[a,c,e,f]
Acousto-optical modulator		
No exit pinhole		
Xiao and Kino (1987)		Castleman (1987)[a]
Nipkow type[d]		
Amos et al. (1987)[c,d,e]		
McCarthy and Walker (1988)	Ellis (1988)	
Nipkow type[d]	Scanned aperture phase contrast[a,c,d]	
Denk *et al.* (1990)		
Two photon[a,c,d,f]		
Hell and Wichmann (1994)		
PSF reduction by stimulated emission depletion[a,b,d]		
		Oldenbourg and Mei (1995)
		LC-pol system[c,d]
Ichihara *et al.* (1996)		
High-throughput spinning disk[d,f,g]		
		Conchello *et al.* (1997)
		Aperture scanning[a,b,c,d,f]
	Gustaffson *et al.* (2000)	
	Structured illumination[a,b,c,d]	
	Volkmer *et al.* (2001)	Inoué *et al.* (2001a,b)
	Coherent anti-stokes raman[c]	Centrifuge pol scope[c,g]
	Inoué *et al.* (2002)	
	Fluorescence pol[c]	

[a] Diffraction theory.
[b] Superresolution.
[c] Contrast modes.
[d] Optical sectioning/depth of field.
[e] Stereo.
[f] 3D in objective space.
[g] High speed.

their intensity distribution in the image must be considered, and resolution generally decreases. The impact of the quality and NA of the condenser on the lateral resolution of point objects was considered by Hopkins and Barham (1950). Their results are similar to, but not strictly identical with, the case of line-grating objects (see Born and Wolf, 1980).

It is important to realize that these resolution criteria apply only to objective lenses used under conditions in which the image is free from significant aberrations (see Chapters 6, 7, 8, 9, 11, and 22, *this volume*; Inoué and Oldenbourg, 1994; Chapters 2 and 3 in Inoué and Spring, 1997). This implies several things:

- A well-corrected clean objective lens is used within the wavelengths of light and diameter of field for which the lens was designed (commonly in conjunction with specific oculars and/or tube lenses).
- The refractive index, dispersion, and thickness of the coverslip and immersion media are those specified for the particular objective lens.
- The correct tube length and ancillary optics are used and the optics are axially aligned.
- The full complement of image-forming rays and light waves leaving all points of the objective-lens aperture converge to the image plane without obstruction.
- The condenser aperture is homogeneously and fully illuminated.
- The condenser is properly focused to produce Köhler illumination.

These considerations for resolution assume that the specimen is viewed in conventional widefield (WF) microscopy. When the (instantaneous) field of view becomes extremely small, as in confocal microscopy, the resolution can in fact be greater than when the field of view is not so limited. We shall return to this point later.[2]

Axial Resolution

We now turn to the axial (z-axis) resolution, measured along the optical axis of the microscope, that is, perpendicular to the plane of focus in which the lateral resolution was considered.

To define axial resolution, it is customary to use the 3D diffraction image of a point source that is formed near the focal plane. In the case of lateral resolution, that is, the resolution in the plane of focus, the Rayleigh criterion makes use of the infocus diffraction images (the central cross-section of the 3D diffraction pattern) of two point sources and the minimum distance that they can approach each other laterally, yet still be distinguished as two. Similarly, axial resolution can be defined by the minimum distance

[2] Note also that one's ability to determine the **location** of an object is not determined by the resolution limit of the system. In fact, the location of an object (diffraction pattern) can be determined under a microscope with precisions that are many times, or even orders of magnitude, greater than the resolution limit (e.g., Denk and Webb, 1987; also see Inoué, 1989).

that the diffraction images of two points can approach each other along the axis of the microscope, yet still be seen as two. To define this minimum distance, we use again the diffraction image of an infinitely small point object and ask for the location of the first minimum along the axis of the microscope.

The precise distribution of energy in the image-forming light above and below focus, especially for high NA objective lenses, cannot be deduced by geometric ray tracing but must be derived from wave optics. The wave optical studies of Linfoot and Wolf (1956) show that the image of a point source produced by a diffraction-limited optical system (e.g., a well-designed and properly used light microscope) is not only periodic around the point of focus in the focal plane, but is also periodic above and below the focal plane along the axis of the microscope. [Such 3D diffraction images (including those produced in the presence of lens aberrations) are presented photographically by Cagnet *et al*. (1962; also see Chapter 7, *this volume*, Fig. 7.4). The intensity distribution calculated by Linfoot and Wolf for an aberration-free system is reproduced in Born and Wolf (1980) and also in Inoué and Spring (1997, Fig. 2-30). The 3D pattern of a point source formed by a lens possessing an annular aperture was calculated by Linfoot and Wolf (1953).]

The distance from the center of the 3D diffraction pattern to the first axial minimum (in object space dimensions) is given by

$$z_{\min} = \frac{2\lambda_o \eta}{(NA_{obj})^2} \qquad \textbf{(3)}$$

where η is the refractive index of the object medium. $z_{\min}$ corresponds to the distance by which we have to raise the microscope objective in order to focus the first intensity minimum observed along the axis of the 3D diffraction pattern instead of the central maximum.[3]

As with the lateral resolution limit, we can use $z_{\min}$ as a measure of the limit of axial resolution of the microscope optics. Note, however, that $z_{\min}$ shrinks inversely proportionally with the *square* of the NA_{obj}, in contrast to the lateral resolution limit which shrinks with the first power of the NA_{obj}. Thus, the ratio of axial-to-lateral resolution ($z_{\min}/r_{Airy} = 3.28\eta/NA_{obj}$) is substantially larger than λ and is inversely proportional to the NA of the objective lens.

Depth of Field

The depth of field of a microscope is the depth of the image (measured along the microscope axis translated into distances in the specimen space) that appears to be sharply in focus at one setting of the fine-focus adjustment. In brightfield microscopy, this depth should be approximately equal to the axial resolution, at least in theory. The actual depth of field has been determined experimentally, and the contribution of various factors that affect the measurement have been explored by Berek (1927).

According to Berek, the depth of field is affected by (1) the geometric and diffraction-limited spreading, above and below the plane of focus, of the light beam that arose from a single point in the specimen; (2) the accommodation of the observer's eye; and (3) the final magnification of the image. The second factor becomes irrelevant when the image is not viewed directly through the ocular but is instead focused onto a thin detector (as in video microscopy or confocal microscopy with a minute exit pinhole). The third factor should also disappear once the total magnification is raised sufficiently, so that the unit diffraction image becomes significantly larger than the resolution element of the detector (e.g., Hansen in Inoué, 1986; Castleman, 1987, 1993; Schotten, 1993; Inoué and Spring, 1997, Section 12.2).

When the detector can be considered to be infinitely thin and made up of resolution elements spaced sufficiently (at least 2-fold) finer than the Airy disk radius, then one need only to consider the diffraction-limited depth of field. In that case, the depth of field is taken to be

$$\delta = \frac{1}{4}(z_{\min^+} - z_{\min^-}) \qquad \textbf{(4)}$$

that is, one quarter of the distance between the first axial minima above ($z_{\min^+}$) and below ($z_{\min^-}$) the central maximum in the 3D Airy pattern converted to distances in specimen space (see Eq. 3; $z_{\min^+}$ and $z_{\min^-}$ correspond to Z1 and −Z1 in Chapter 7, Fig. 7.4, *this volume*).

In conventional fluorescence and darkfield microscopy, the light arising from each image point produces significant intensity within a solid cone that reaches a considerable distance above and below focus (as seen in the point-spread functions for these modes of microscopy; e.g., Streibl, 1985; also Chapters 11 and 23, *this volume*). Therefore, fluorescent (or light-scattering) objects that are out of focus produce unwanted light that is collected by the objective and reduces the contrast of the signal from the region in focus.

For these reasons, the depth of field may be difficult to measure or even to define precisely in conventional fluorescence and darkfield microscopy. Put another way, one could say that when objects that are not infinitely thin are observed in conventional fluorescence or darkfield microscopy, the apparent depth of field is very much greater than the axial resolution.

The unwanted light that expands the apparent depth of field is exactly what confocal imaging eliminates. Thus, we can view only those fluorescent and light-scattering objects that lie within the depth that is given by the axial resolution of the microscope and attain the desired shallow depth of field.

As mentioned earlier, the lateral resolution of a microscope is also a function of the size of the field observed at any one instant. Tolardo di Francia (1955) suggested, and Ingelstam (1956) argued on the basis of information theory, that one gains lateral resolution by a factor of $\sqrt{2}$ as the field of view becomes vanishingly small. These theoretical considerations set the stage for the development of confocal imaging.

CONFOCAL IMAGING

As a young postdoctoral fellow at Harvard University in 1957, Marvin Minsky applied for a patent for a microscope that used a stage-scanning confocal optical system. Not only was the conception farsighted, but his insight into the potential application and significance of confocal microscopy was nothing short of remarkable. [See the delightful article by Minsky (1988) that shows even greater insight into the significance of confocal imaging than do the following extracts culled from his patent application.]

In Minsky's embodiment of the confocal microscope, the conventional microscope condenser is replaced by a lens identical to the objective lens. The field of illumination is limited by a pinhole, positioned on the microscope axis. A reduced image of this pinhole

[3] As discussed later, the distance $z_{\min}$ can be reduced significantly below the classical limit given by Eq. 1.3, for example, by reducing the effective point-spread function by special use of two-photon confocal imaging.

is projected onto the specimen by the "condenser." The field of view is also restricted by a second (or exit) pinhole in the image plane placed confocally to the illuminated spot in the specimen and to the first pinhole (Fig. 1.1). Instead of trans-illuminating the specimen with a separate "condenser" and objective lens, the confocal microscope could also be used in the epi-illuminating mode, making a single objective lens serve as both the condenser and the objective lens (Fig. 1.2).

Using either transmitted or epi-illumination, the specimen is scanned with a point of light by moving the specimen over short distances in a raster pattern. (The specimen stage was supported on two orthogonally vibrating tuning forks driven by electromagnets at 60 and 6000 Hz.) The variation in the amount of light, modulated by the specimen and passing the second pinhole, is captured by a photoelectric cell. The photoelectric current is amplified and modulates the beam intensity of a long-persistence cathode-ray tube (CRT) scanned in synchrony with the tuning forks. As a result, the image of the specimen is displayed on the CRT. The ratio of scanning distances between the electron beam and the specimen provides image magnification, which is variable and can be very large.

With this stage-scanning confocal microscope, Minsky says, light scattered from parts other than the illuminated point on the specimen is rejected from the optical system (by the exit pinhole) to an extent never before realized. As pointed out in the patent application, there are several advantages to such an optical system:

- Reduced blurring of the image from light scattering
- Increased effective resolution
- Improved signal-to-noise ratio
- Permits unusually clear examination of thick, light-scattering objects
- *xy*-scan possible over wide areas of the specimen
- Inclusion of a *z*-scan is possible
- Electronic adjustment of magnification

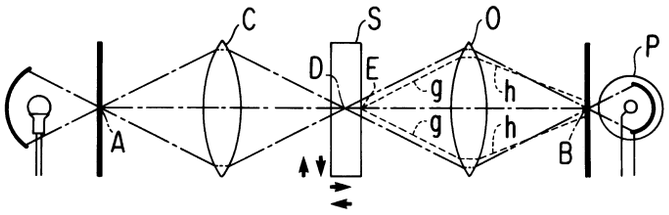

FIGURE 1.1. Optical path in simple confocal microscope. The condenser lens, C, forms an image of the first pinhole, A, onto a confocal spot, D, in the specimen, S. The objective lens, O, forms an image of D onto the second (exit) pinhole, B, which is confocal with D and A. Another point, such as E in the specimen, would not be in focus with A, so that the illumination would be less. In addition, most of the light, g–h, scattered from E would not pass the second pinhole, B. The light reaching the phototube, P, from E is thus greatly attenuated compared to that from the confocal point, D. In addition, the exit pinhole can be made small enough to exclude the diffraction rings in the image of D, so that the resolving power of the microscope is improved. As the specimen is scanned, the phototube provides a signal of the light passing through sequential specimen points D_1, D_2, D_3, etc. (not shown). D_1, D_2, D_3, etc., can lie in the focal plane as in conventional microscopy or perpendicular to it, or at any angle defined by the scanning pattern, so that optical sections can be made in or at angles tilted from the conventional image plane. Because, in the stage-scanning system, the small scanning spot, D, lies exactly on the axis of the microscope, the lenses C and O can be considerably less sophisticated than conventional microscope lenses, which must form images from points some distance away from the lens axis. (After Minsky, 1957.)

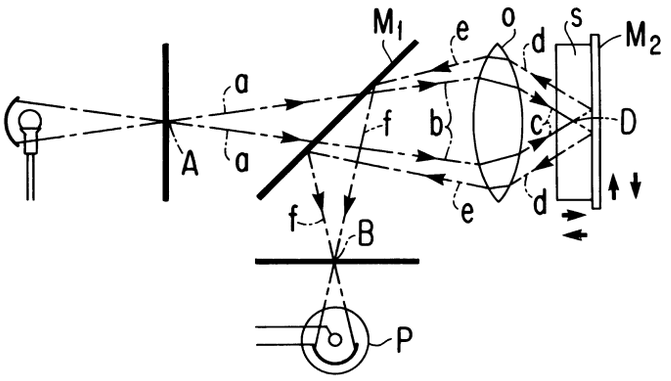

FIGURE 1.2. Optical path in epi-illuminated confocal microscope. The entrance pinhole, A, point D in the specimen, S, and exit pinhole, B, are confocal points as in Figure 1.1. A partial, or dichromatic, mirror, M_1, transmits the illuminating beam a–b–c and reflects the beam d–e which passed D and was reflected by the mirror, M_2, on which the specimen is lying. Only the reflected beam that passes point D focuses onto the detector pinhole and reaches the photocell, P. A single lens, O, replaces the condenser and objective lenses in Figure 1.1. (After Minsky, 1957.)

- Especially well suited for making quantitative studies of the optical properties of the specimen
- An infinite number of aperture planes in the microscope are potentially available for modulating the aperture with darkfield stops, annuli, phase plates, etc.
- Complex contrast effects can be provided with comparatively simple equipment
- Permits use of less complex objective lenses, including those for long working distance, ultraviolet (UV), or infrared imaging, as they need to be corrected only for a single axial point.

The high-resolution acoustic microscope developed by Quate and co-workers (Quate, 1980) and the laser disk, video, and audio recorder/players are object-scanning-type confocal microscopes. The designers of these instruments take advantage of the fact that only a single axial point is focused or scanned (see, e.g., Inoué and Spring, 1997, Sect. 11.10).

IMPACT OF VIDEO

Nipkow Disk

Just about the same time that Abbe in Jena laid the foundation for modern light microscopy, a young student in Berlin, Paul Nipkow (1884), figured out how to convert a two-dimensional (2D) optical image into an electrical signal that could be transmitted as a one-dimensional (1D), or serial, time-dependent signal, over a single cable (as in a Morse code). Prior to Nipkow, most attempts at the electrical transmission of optical images involved the use of multiple detectors and as many cables.

Nipkow dissected the image by scanning over it in a raster pattern, using a spinning opaque wheel perforated by a series of rectangular holes. The successive holes, placed a constant angle apart around the center of the disk but on constantly decreasing radii (i.e., arranged as an Archimedes spiral), generated the raster-scanning pattern (Fig. 1.3). The brightness of each image element, thus scanned by the raster, was picked up by a photocell. The

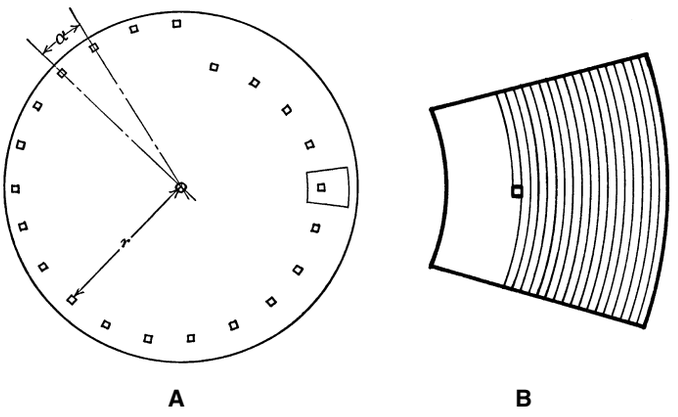

FIGURE 1.3. Nipkow disk. The perforations in the opaque disk, A, which is rotating at a constant velocity, scan the image in a raster pattern as shown in B. (After Zworykin and Morton, 1954.)

output of the photocell reflected the brightness of the sequentially scanned image elements and drove a neon bulb that, viewed through another (part of the) Nipkow disk, reproduced the desired picture.

A similar type of scanner disk, but with multiple, centrosymmetric sets of spirally placed holes, was used by Mojmir Petráň and co-workers at Prague and New Haven to develop their epi-illuminated tandem-scanning confocal microscope (TSM) (Egger and Petráň, 1967; Petráň *et al*., 1968). In Petráň's microscope, holes on a portion of the spinning disk placed in front of the light-source collector lens are imaged onto the specimen by the objective lens. Each point of light reflected or scattered by the specimen is focused by the same objective lens back onto the centrosymmetric portion of the Nipkow disk. The pinholes at this region exclude the light originating from points in the specimen not illuminated by the first set of pinholes, giving rise to confocal operation (Chapter 10, *this volume*).

As with Nipkow's initial attempt at television, this TSM tends to suffer from the low fraction (1%–2%) of light that is transmitted through the source pinholes. Also, very high mechanical precision is required for fabricating the symmetrical Nipkow disk and for spinning it exactly on axis. In addition, some of the advantages pointed out by Minsky for the stage-scanning type confocal optics are lost because the objective lenses are no longer focusing a single axial point of light.

However, for biological applications, the tandem-scanning system provides the decided advantage that the specimen remains stationary. As a result, the speed of the raster scan is not limited by the mass of the specimen support as it is in stage scanning, and the scanning system is unlikely to introduce any geometrical distortion. Thus, with a TSM, one can observe objects that reflect or scatter light moderately strongly, in real time, either by using a television or photographic camera or by observing the image directly through the eyepiece.

In addition to Petráň and co-workers, Alan Boyde (1985a) in London took advantage of the good axial discrimination and light-penetrating capability of the tandem scanning confocal microscope and pioneered its use for viewing biological objects. In particular, he used it for imaging below the surface of hard tissue such as bone and teeth to visualize the cells and lacunae found there (see Lewin, 1985). Boyde also provides striking stereoscopic images obtained with the tandem-scanning confocal microscope (Boyde, 1985b, 1987).

Gordon Kino and co-workers at Stanford University have designed a confocal microscope using a Nipkow disk in a manner that differs somewhat from the Petráň type (Xiao and Kino, 1987; also see Chapter 10, *this volume*). In the Kino type, the rays illuminating the specimen and those scattered by the specimen traverse the *same* set of pinholes on the spinning Nipkow disk rather than those that are centrosymmetrical. By using a special low-reflection Nipkow disk, tilted somewhat to the optic axis of the microscope, and by employing crossed polarizers and a quarter-wave birefringent plate to further reduce the spurious reflections from the disk, they are able to use only one side of it, thus alleviating some of the alignment difficulties of the Petráň type.

More recently, spinning-disk confocal units have been vastly improved by adding microlenses to the pinholes. As described later (see "Yokogawa Disk-Scanning Confocal System" below), the microlens-equipped disk-scanning systems effectively provide video-rate and faster confocal full-frame imaging and in real color. While in part depending on older technology, the confocal-scanning unit (CSU) systems turn out to have certain advantages not achievable with point-scanning confocal systems.

Electron-Beam-Scanning Television

While Nipkow's invention laid the conceptual groundwork for television, raster scanning based on a mechanical device was simply too inefficient for practical television. Thus, it was not until five decades after Nipkow, following the advent of vacuum tube and electronic technology, that Zworykin (1934) and his colleagues at RCA were able to devise a practical television system. These workers developed the image iconoscope, an image-storage-type electron-beam-scanning image pickup tube. The image iconoscope, coupled with a CRT for picture display, permitted very rapid, "inertialess" switching and scanning of the image and picture elements. With these major breakthroughs, television not only became practical for broadcasting but emerged as a tool that could be applied to microscopy (see Inoué and Spring, 1997, Sects. 1.1 and 1.2).

An early application of video (the picture portion of television) was the flying spot UV microscope of Young and Roberts (1951). With this microscope, the specimen remains stationary and single object points are scanned serially in a raster pattern by a moving spot of UV light emitted by the face of a special high-intensity UV-CRT. The optical elements (condenser) of the microscope demagnify this moving spot onto the specimen, which modulates its brightness. The modulated UV light is then picked up by a phototube and amplified electronically before being displayed on a visible-light CRT scanned in synchrony with the UV-CRT.

Young and Roberts point out that by illuminating only a single specimen point at a time with a flying-spot microscope, flare is reduced and the image becomes a closer rendition of the specimen's optical properties than that obtained with a non-scanning microscope. They also point out that for these same reasons — and because a photoelectric detector can provide a sequential, linear output of the brightness of each specimen point — quantitative analysis becomes possible with a flying-spot microscope. In addition, they note that the electronic photodetector raises the sensitivity of image capture by perhaps two orders of magnitude compared to photography.

It should be noted that the flare which would otherwise arise from the unilluminated parts of the specimen is significantly

reduced with a flying-spot microscope (see Sheppard and Choudhury, 1977), even though the exit pinhole used in a confocal microscope is not present. Thus, for example, Wilke *et al*. (1983) and Suzuki and Hirokawa (1986) developed laser-scanning flying-spot microscopes (coupled with digital image processors) to raise image contrast (at video rate) in fluorescence, differential-interference-contrast (DIC), and brightfield microscopy. Naturally, the exit pinhole in a confocal system is very much more effective at excluding unwanted light arising from different layers or portions of the specimen not currently illuminated by the source "pinhole," but it does so at the cost of reduced image brightness, lower scanning speed, and increased instrumental complexity and price.

While the flying-spot, or beam-scanning, microscope was developed and applied in UV microscopy for about a decade after its introduction, its further development as an imaging device was eclipsed for some time by the need and the opportunity to develop automated microscopy for rapid cell sorting and diagnosis. Here, the aim was not the imaging of cell structures as such but rather the rapid and efficient classification of cells based on their biochemical characteristics, taking advantage of the emerging power of high-speed digital computers. The size, shape, absorbance, light scattering, or light emission of cells (labeled with specific fluorescent markers) was used either to classify the cells by scanning the slide under a microscope or to sort the cells at very high rates as the cells traversed a monitoring laser beam in a flow cell or a Coulter-type cell separator.

Impact of Modern Video

Meanwhile, starting in the late 1970s, the introduction of new solid state devices, especially large-scale integrated circuits and related technology, led to dramatic improvements in the performance and availability, and reduction in price, of industrial-grade video cameras, video tape recorders, and display devices. Concurrently, ever more compact and powerful digital computers and image-processing systems appeared in rapid succession. These advances led to the birth of modern video microscopy, which in turn brought about a revitalized interest in the power and use of the light microscope (for reviews see Allen *et al*., 1981a,b; Inoué, 1981, 1989; Allen, 1985; Inoué and Spring, 1997).

In brief, dynamic structures in living cells could now be visualized with a clarity, speed, and resolution never achieved before in DIC, fluorescence, polarized-light, darkfield, and other modes of microscopy; the growth and shortening of individual molecular filaments of tubulin and f-actin, and their gliding motion and interaction with motor molecules, could be followed in real time directly on the monitor screen; and the changing concentration and distribution of ions and specific protein molecules tagged with fluorescent reporter molecules could be followed, moment by moment, in physiologically active cells (Chapters 19, 29, and 42, *this volume*).

In addition to its immediate impact on cellular and molecular biology, video microscopy and digital image processing also stimulated the exploration of other new approaches in light microscopy along several fronts. These include the development of ratio imaging and new reporter dyes for quantitative measurement of local intracellular pH, calcium ion concentration, etc. (Tanasugarn *et al*., 1984; Bright *et al*., 1989; Tsien, 1989; Chapters 16, 19, and 29, *this volume*); the computational extraction of pure optical sections from whole-mount specimens in fluorescence microscopy (based on deconvolution of multi-layered images utilizing knowledge of the microscope's point-spread function; Agard and Sedat, 1983; Agard *et al*., 1989; see also Chapters 23, 24, and 25, *this volume*); 3D imaging including stereoscopy (Brakenhoff *et al*., 1986, 1989; Inoué and Inoué, 1986; Åslund *et al*., 1987; Stevens *et al*., 1994; Inoué and Spring, 1997, Sect. 12.7.7); and, finally, the further development of laser-scanning microscopy and confocal microscopy.

LASERS AND MICROSCOPY

Holography

In 1960, Maiman announced the development of the first operating laser. However, "his initial paper, which would have made his findings known in a more traditional fashion, was rejected for publication by the editors of *Physical Review Letters* — this to their everlasting chagrin." (For historic accounts including this quotation and a comprehensive discussion of the principles and application of lasers and holography, see Sects. 14.2 and 14.3 in Hecht, 1987; see also Chapter 5, *this volume*.) Shortly thereafter, two types of applications of lasers were sought in microscopy. One took advantage of the high degree of monochromaticity and the attendant long coherence length. Coherence length is the distance over which the laser waves could be shifted in path and still remain coherent enough to display clear interference phenomena (note that, in fact, this reflects a very high degree of temporal coherence). These characteristics made the laser an ideal source for holography (Leith and Upatnieks, 1963, 1964).

To explore the use of holography with the microscope, Ellis (1966) introduced a conventional light microscope into one of two beams split from a laser. When this beam was combined with the other beam passing outside of the microscope, the two beams could be made to interfere in a plane above the ocular. The closely spaced interference fringes were recorded on very fine-grained photographic film to produce the hologram.

What Ellis found was that the coherence length of the laser beam was so long that the hologram constructed as described above could be viewed not only to reconstruct an image of the specimen being magnified by the microscope, but also to reconstruct images of the inside of the microscope. Indeed, in the hologram one could see the whole optical train and interior of the microscope, starting with the substage condenser assembly, the specimen, the objective lens and its back aperture, the interior of the body tube up to the ocular, and even the light shield placed above it! This made it possible for Ellis to view the hologram through appropriately positioned stops, phase plates, etc., and to generate contrast from the specimen in imaging modes such as darkfield or oblique illumination, phase contrast, etc., *after* the hologram itself had been recorded. In other words, the state of the specimen at a given point of time could be reconstructed and viewed after the fact in contrast modes different from the one present when the hologram was recorded.

In principle, holomicrography presents many intriguing possibilities including 3D imaging. But the very virtue of the long coherence length of the laser beam means that the hologram also registers all the defects and dirt in the microscope. Without laser illumination, the optical noise produced by these defects would be far out of focus. With a laser illuminating the whole field of view of the microscope, the interference fringes from these out-of-focus defects intrude into the holographic image of the specimen where they are prominently superimposed. Because of this problem, holomicrography has so far not been widely used. [However, see

Sharnoff *et al*. (1986), who have figured out how to obtain holomicrograms that display only the *changes* taking place in the specimen (contracting muscle striations) over an interval of time and thus eliminate the fixed-patterned optical noise.]

Laser Illumination

Another practical application of lasers in microscopy is its use as an intense, monochromatic light source. Lasers can produce light beams with a very high degree of monochromaticity and polarization, implying a high degree of coherence. Some lasers also generate beams with very high intensity. Thus, an appropriate laser could serve as a valuable light source in those modes of microscopy where monochromaticity, high intensity, and a high degree of coherence and polarization are important.

To use the laser as an effective light source for microscopy, three conditions must be satisfied:

- Both the microscope's field of view and the condenser aperture must appropriately be filled.
- The coherence length of the laser beam (i.e., the temporal coherence) must be reduced to eliminate interference from out-of-focus defects.
- The coherence at the image plane must be reduced to eliminate laser "speckle" and to maximize image resolution.

In fact, these three conditions are not totally independent, but they do specify the conditions that must be met.

One of the following five approaches can be used to fulfill these conditions (see also Chapter 6, *this volume*).

Spinning-Disk Scrambler

The laser beam, expanded to fill the desired field, is passed through a spinning ground-glass diffuser placed in front of the beam expander lens (Hard *et al*., 1977). The ground glass diffuses the light so that the condenser aperture is automatically filled. However, if the ground glass were not moving, small regions of its irregular surface would act as coherent scatterers and the image field would still be filled with laser speckle. Spinning or vibrating the ground glass reduces the temporal coherence of each of the coherent scattering points to a period shorter than the integration time of the image sensor. Thus, when averaged over the period of the motion, the field also becomes uniformly illuminated. This approach, while simple to understand, can result in considerable light loss at the diffuser. Also, inhomogeneity of the diffuser's texture can give rise to concentric rings of varying brightnesses which traverse the field.

Oscillating-Fiber Scrambler

The laser beam is focused onto the entrance end of a single-stranded multi-mode optical fiber whose output end lies at the focal point of a beam-expanding lens. This lens projects an enlarged image of the fiber tip to fill the condenser aperture. The fiber, which is fixed at both ends, is vibrated at some point along its length. The field and aperture are then uniformly filled with incoherent light with little loss of intensity (Ellis, 1979). If the fiber were not vibrated, the simple fact that the light beam is transmitted through the fiber could make the laser beam highly multi-modal. That would reduce the lateral coherence of the beam at the aperture plane, but the image would still be filled with speckle. Vibration that reduces the temporal coherence of the beam below the integration time of the image sensor integrates out the speckle without loss of light (see also Chapter 6, *this volume*).

Multi-Length Fiber Scrambler

None of the mechanical scramblers mentioned above can be used where speckles have to be removed within extremely brief time periods. For example, in a centrifuge polarizing microscope, the laser output must be made spatially incoherent within the few nanoseconds required to freeze the image of the specimen flying through the field of the objective lens at speeds up to 100 m/s (Inoué *et al*., 2001b). Our solution for reducing the coherence of the laser pulse was to introduce a fiber bundle made up of up to 100 fibers of multiple lengths between two multi-mode single-fiber scramblers. The first multi-mode fiber introduced some phase randomizing effects, while the multi-length fibers provided a fiber bundle output whose phase varied depending on the length of the fiber. However, the intensities of the fiber output varied depending on their location in the bundle. The final multi-mode fiber made the non-uniform brightness of the bundle output homogeneous, so that the microscope condenser received uniform illumination. Thus, without using any mechanically moving parts, the phase of the monochromatic laser beam is randomized, and speckles are eliminated from the field image, while the whole condenser aperture is filled uniformly.

Field Scanning

The field is scanned by a minute focused spot (the diffraction image) of a single-mode laser beam that has been expanded to fill the condenser aperture (as in a laser-scanning confocal microscope). Thus, the specimen is scanned point by point, and the signal light reflected, transmitted, or emitted by the specimen is collected and focused by the objective lens. This imaging mode avoids the generation of speckle from laser-illuminated specimens because speckle arises from the interference between the coherent light waves scattered from different parts of a specimen. (This optical setup is less effective at removing speckle when a smooth reflecting surface is presented slightly away from the plane of focus.)

This fourth approach leads to field-scanning microscopy. A focused spot of laser light can be made to scan the field as in a flying-spot microscope, or the specimen can be moved and scanned through a fixed focus point. Alternatively, an exit pinhole and beam scanners can be added to generate a laser-scanning confocal microscope.

Aperture Scanning

The minute diffraction image of a single-mode laser is focused by a beam expander onto an off-axis point on the condenser aperture. The small spot is scanned (made to precess) over the condenser aperture in such a way that the field is uniformly illuminated. At any instant of time, the specimen is illuminated by a tilted collimated beam of light emerging from the condenser and originating from the illuminated aperture point. Selected regions of the aperture are filled in rapid succession by scanning the spot, so that the whole field is illuminated by collimated, coherent beams at successively changing azimuth angles. The rapid scanning of the source reduces the temporal coherence of illumination at the object plane to less than the response time of the image detector. Nevertheless, the lateral coherence is maintained for each instantaneous beam that illuminates the specimen (Ellis, 1988).

Ellis has argued the theoretical advantage provided by this fifth approach and has demonstrated its practical attractiveness. With aperture scanning, one gains new degrees of freedom for optical image processing because the aperture function (which controls the image transfer function of the microscope) can be regulated dynamically for each point of the aperture. The image resolution

and the shallow depth of field that can be achieved with aperture-scanning phase-contrast microscopy is most impressive (see, e.g., Inoué and Spring, 1997, Fig. 2-47).

Laser-Illuminated Confocal Microscopes

During the early 1970s, Egger and co-workers at Yale University developed a laser-illuminated confocal microscope in which the objective lens was oscillated in order to scan the beam over the specimen. Davidovits and Egger obtained a U.S. patent on this microscope (1972; see review by Egger, 1989).

A few years later, Sheppard and Choudhury (1977) provided a thorough theoretical analysis on various modes of confocal and laser-scanning microscopy. The following year, Sheppard *et al*. (1978) and Wilson *et al*. (1980) described an epi-illuminating confocal microscope of the stage-scanning type, equipped with a laser source and a photomultiplier tube (PMT) as the detector, using a novel specimen holder. The specimen holder, supported on four taut steel wires running parallel to the optical axis, allowed precise *z*-axis positioning as well as fairly rapid voice-coil-actuated scanning of the specimen in the *xy*-plane. Using this instrument, Sheppard *et al*. demonstrated the value of the confocal system particularly for examining integrated circuit chips. With stage-scanning confocal imaging, optical sections and profile images could be displayed on a slow-scan monitor over areas very much *larger* than can be contained within the field of view of any given objective lens by conventional microscopy.

These authors capitalized on the fact that the confocal signal falls off extremely sharply with depth, and the image is therefore completely dark for regions of the specimen that are not near the confocal focus plane. For example, with a tilted integrated circuit chip, only the portion of the surface within the shallow depth of field (at any selected *z*-value) could be displayed, as a strip-shaped region elongated parallel to the chip's axis of tilt. Other areas of the image were dark and devoid of structure. Conversely, by combining all the *xy*-scan images made during a slow *z*-scan, they could produce a final "extended focus" image of the whole tilted surface, which demonstrated maximum spatial resolution on all features throughout the focus range (Wilson and Sheppard, 1984; Wilson, 1985) (Chapter 22, *this volume*).

This could be done even when the specimen surface was not a single tilted plane but was wavy or consisted of complex surfaces. In their monograph *Scanning Optical Microscopy*, Wilson and Sheppard (1984) show shallow optical sections of insect antennae shining on a dark background. They also show stereo-pair images of the same object consisting of two "extended focus" images made by focusing along two focal axes that were tilted by several degrees relative to the optical axis. Extended-focus images demonstrate that *the confocal system can either decrease or increase the effective depth of field without loss of resolution*.

As described in the final section of this article, the lateral resolution that is practically attainable can be improved by using confocal optics. In addition, the removal of the extraneous light contributed by out-of-focus objects dramatically improves the contrast and gives rise to a brilliantly sharp image.

Sheppard *et al*. also managed to display different regions on the surface of an integrated circuit chip with varying intensity or pseudocolor corresponding to the height of the region. This is possible because the amount of light reflected by an (untilted) step on the surface of the chip and passing the second pinhole varies with the distance of the reflecting surface from the focal plane. The authors also showed that, by processing the photoelectric signal electronically, the edges of the steps alone could be outlined or the gradient of the steps could be displayed in a DIC-like image (Hamilton and Wilson, 1984). [For the basics of digital image processing, see Castleman (1979), Baxes (1984), Gonzales and Wintz (1987), Chapter 12 in Inoué and Spring (1997), and Chapter 14, *this volume*.]

The integrated circuit chip could also be displayed with contrast reflecting the status of the local circuit elements, for example, reflecting its temperature or the amount of photo-induced current flowing through the circuit, superimposed on the confocal image of the chip made with reflected light (Wilson and Sheppard, 1984).

In addition to the Oxford group, the brothers Cremer and Cremer (1978) of Heidelberg designed a specimen-scanning laser-illuminated confocal microscope. This epi-fluorescence system was equipped with (1) a circular exit pinhole, in front of the first PMT, whose diameter was equal to the principal maximum of the diffraction pattern; and (2) an annular aperture, in front of a second PMT, whose opening corresponded to the first subsidiary maximum of the diffraction pattern. The output of the two PMTs was used to provide autofocus as well as displays of surface contour and fluorescent intensity distribution.

In the 1978 article, the Cremers also discussed the possibility of laser spot illumination using a "4π-point hologram" that could, at least in principle, provide long working distance relative to the small spot size that could be produced.

CONFOCAL LASER-SCANNING MICROSCOPE

In addition to those already mentioned, the pioneering work of the Oxford electrical engineering group was followed in several European laboratories by Brakenhoff *et al*. (1979, 1985), Wijnaendts van Resandt *et al*. (1985), and Carlsson *et al*. (1985). These investigators respectively developed the stage-scanning confocal microscope further, verified the theory of confocal imaging, and expanded its application into cell biology. I shall defer further discussions on these important contributions to authors of other chapters in this volume. In the meantime, video microscopy and digital image processing were also advancing at a rapid rate.

These circumstances culminated in the development of the confocal laser-scanning microscope (CLSM, Figs. 1.4, 1.5; Åslund *et al*., 1983, 1987) and publication of its biological application by Carlsson *et al*. (1985), Amos *et al*. (1987), and White *et al*. (1987). The publications were followed shortly by introduction of laser-scanning confocal microscopes to the market by Sarastro, Bio-Rad, Olympus, Zeiss, and Leitz. It was White, Amos, and Fordham of the Cambridge group that first enraptured the world's biological community with their exquisite and convincing illustrations of the power of the CLSM. Here at last was a microscope that could generate clear, thin optical sectioned images, totally free of out-of-focus fluorescence, from whole embryos or cells and at NAs as high as 1.4. Not only could one obtain such remarkable optical-sectioned fluorescence images in a matter of seconds, but *x-z* sections (providing views at right angles to the normal direction of observation) could also be captured and rapidly displayed on the monitor. A series of optical sections (stored in the memory of the built-in or add-on digital image processor) could be converted into 3D images or displayed as stereo pairs. The confocal fluorescent optical sections could also be displayed side by side with non-confocal brightfield or phase-contrast images, acquired concurrently using the transmitted portion of the scanning laser beam. These images could also be displayed superimposed on top of each other, for example, with each image coded in different pseudocolor, but unlike similar image pairs produced by conventional

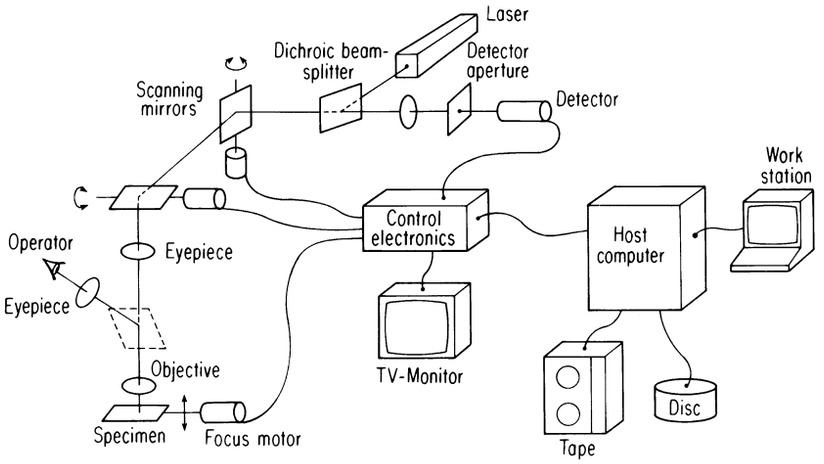

FIGURE 1.4. Schematic of laser-scanning confocal microscope. (From Åslund *et al*., 1987.)

microscopes, the two images were in exact register and showed no parallax as each was generated by the same scanning spot.

Most of the laser-scanning systems discussed in this section employed epi-illumination using some form of mechanical scanning devices. They could not readily be applied to confocal imaging of transmitted light, for example, for high-extinction polarization or DIC microscopy. Nevertheless, Goldstein *et al*. (1990) developed a system using an Image Dissector Tube which, in principle, should be able to provide confocal imaging in the trans-illumination mode. Such an approach may eventually lead to workable transmission laser-scanning confocal microscopes with multiple contrast modes.

TWO- AND MULTI-PHOTON MICROSCOPY

As noted, conventional point-scanning confocal microscopes dramatically reduce the contribution of fluorescence from out-of-focus regions of the specimen. Nevertheless, regions of the specimen above and below the focal plane are exposed to the full cones of intense excitation light, converging and diverging from the illuminated spot. Thus, with conventional confocal microscopy, biological specimens tend to suffer from photon-induced damage and rapid bleaching of fluorescence, while the fraction of the short wavelength excitation beam that reaches the focal plane is reduced by absorption in the intervening material. Many of these shortcomings are circumvented by two- and multi-photon microscopy.

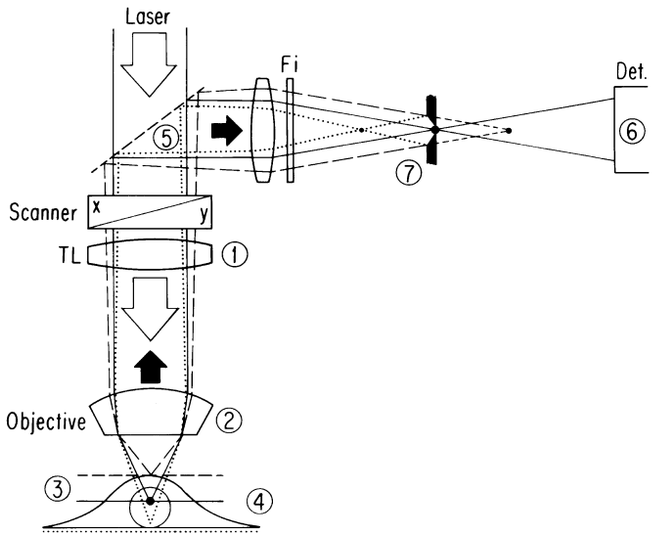

FIGURE 1.5. Depth discrimination in a laser-scanning confocal fluorescent microscope. Compare with Figure 1.2. (Courtesy of Dr. H. Kapitza, Carl Zeiss, Oberkochen.)

By focusing a pulse of very intense laser beam with twice the wavelength (half the frequency) of the standard short wavelength excitation beam, and within a period shorter than the fluorescence decay time of the fluorophore, the coherently interfering photons can excite molecules at half the wavelength of the long wavelength laser, and do so *selectively* in the focused spot. In other words, the output of an intense near-infrared (IR) laser induces fluorescence in a blue or UV excitable fluorophore at, and only at, the focused spot where the coherent electromagnetic field strength is so high (within the required brief period) that it acts nonlinearly to excite the chromophores at twice the frequency of the IR field. The fluorophores in the cone of the illuminating light above and below focus do not experience the two-photon effect and, therefore, are not excited or damaged. Additionally, in contrast to conventional confocal microscopy, two-photon laser scanning systems do not require an exit pinhole or an image-forming objective lens. This is because the minute two-photon excited fluorescent spot is totally isolated in space and is free of "parasitic" fluorescence in the *xy*-plane as well as along the *z*-axis. Therefore, the fluorescence emission needs only to be collected by an efficient photodetector as the excitation spot is being scanned (see Chapter 28, *this volume*).

Thus, compared to conventional confocal microscopy, two-photon microscopy permits confocal imaging of planes much deeper in the tissue, and with considerably higher light-gathering efficiency, as well as with less fluorescence bleaching and specimen damage outside of the focal plane. Denk *et al*. (1990) and Squirrel *et al*. (1999) have made extended time-lapse recordings of dividing tissue-cultured cells and mammalian embryos in two-photon microscopy.

In another interesting and ingenious application of two-photon microscopy, the fluorescence excitation volume (point-spread function) has been reduced considerably below that defined by wave optics by use of two partially overlapping excitation volumes. The first excites fluorescence in the standard two-photon volume, while the second volume, concurrently generated by a somewhat longer wavelength, quenches the fluorescence (by stim-

ulated emission depletion) in the zone where the two volumes overlap each other. A phase plate in the depletion beam path has the effect that this beam is almost the inverse of the Airy disk and has a null at the focus. Thus, the volume of region actually fluorescing is carved smaller than the standard two-photon excitation volume, and, in fact, Hell and Wichmann (1994) report having reduced the height of the point-spread function (PSF) by as much as a factor of five (see also Klar *et al.*, 2000, Chapter 31, *this volume*).

IS LASER-SCANNING CONFOCAL MICROSCOPY A CURE-ALL?

With the impressively thin and clean optical sections that are obtainable, and the *x*-*z* sections and stereoscopic images that can neatly be displayed or reconstructed, one can be tempted to treat the CLSM as a cure-all. One may even think of the instrument as the single microscope that should be used for all modern cell biology or embryology. How valid is such a statement and what, in fact, are the limitations of the current instruments beyond their high costs?

The fundamental limits of confocal imaging will be covered in the next chapter. Here I will comment on three topics: the speed of image or data acquisition, comparison with the depth of field in phase-dependent imaging, and some optical and mechanical factors affecting confocal microscopy.

Speed of Image or Data Acquisition

Several factors affect the time needed to acquire a usable image with a confocal microscope. These include (1) the type of confocal system used; (2) the optical magnification and numerical aperture of the system; (3) the desired area covered; (4) required quality of the image (e.g., lateral and axial resolution, levels of image gray scale, degree of freedom from graininess); and (5) the amount of light reaching the sensor. Here we will survey a few general points relating to the choice of instruments, specifically as applied to biology.

Among the different confocal systems, the stage-scanning type requires the longest time (~10 s) to acquire a single image because the specimen support has to be translated (vibrated) very precisely. Biological specimens are often bathed in a liquid medium, and for these, any movement presents a problem. Even if the specimen chamber is completely sealed and the gas phase excluded to minimize the inertial effects of stage scanning, specimen motion still can occur during stage scanning. The alternative lens-scanning system can encounter worse problems when oil-immersion lenses are used. Very often structures in biological specimens are moving or changing dynamically at rates incompatible with very slow scan rates. Thus, despite the many virtues of the stage-scanning system recognized by Minsky (1957) and by Wilson and Sheppard (1984), there is little chance that the stage-scanning microscope will be widely used in biology. An exception might be for large-area 3D scanning of fixed and permanently mounted specimens. Such specimens require, or can take advantage of, those virtues of the stage-scanning system that cannot be duplicated by other confocal designs.

In the Petráň-type TSM or the Kino-type confocal microscope, the disk can be spun rapidly enough to provide images at video rate (30 frames/s). When speed of image acquisition is of paramount importance, as in the study of moving cells, living cells at high magnification, or microtubules growing *in vitro*, the type of speed provided by the Nipkow disk system may be indispensable. For example, at the ~10,000× magnification needed for clear visualization, the Brownian motion of microtubules (even those many micrometers long) is so great that an image acquisition time of >0.1 s blurs the image beyond use.

As discussed earlier, the downside of the classical Nipkow disk-type system is that the efficiency of light transmission is low, light reflected by the spinning disk reduces image contrast, and the image may suffer from intrusive scan lines. Also, observation is usually by direct viewing through the ocular, or via some photographic or video imaging device, rather than using a PMT. While video imaging does have its own advantages, video sensors other than cooled charge-coupled devices (CCDs) and special return-beam-type pickup tubes operate over a limited dynamic range. Conventional video pickup tubes seldom respond linearly over a range of >100 : 1 (more commonly somewhat less; see Inoué and Spring, 1997), and they have relatively high measurement noise. By contrast, a PMT can have a dynamic range of $\geq 10^6$. When exceedingly weak signals need to be detected from among strong signals, or when image photometry demands dynamic range and precision beyond those attainable with standard video cameras, an imaging system using a cooled CCD or a PMT detector may be required. Modern stage-scanning- and laser-scanning-type confocal microscopes use such detectors (Chapter 12, *this volume*). Nevertheless, for some applications improved versions of the Nipkow-disk-type confocal instruments may provide optical sections with better signal and image quality than with CLSMs as discussed below under "Yokogawa Disk-Scanning Confocal System."

The frame-scanning rate of the CLSM falls somewhere between that of the stage- and tandem-scanning types, normally about 1 to 2 s/frames. This rate is the minimum time required by the mirror galvanometers (that are used to scan the illuminating and return beams) to produce an image of, say, 512×768 picture elements. This limitation in scanning speed relates to the absolute time required to scan along the fastest axis (usually the *x*, or horizontal, scan). The scanning speed cannot be increased without affecting image resolution or confocal discrimination (Chapters 3, 21, and 25, *this volume*).

The *x*-scanning speed can be increased by using a resonance galvanometer, a spinning mirror, or an acousto-optical modulator instead of the mirror galvanometers (Chapters 3, 9, and 29, *this volume*). However, doing so may reduce both scan flexibility (i.e., no optical "zoom" magnification) and inefficient use of the duty cycle. Furthermore, in a scanning confocal system used for fluorescence microscopy, one cannot use the same acousto-optical device (or other diffraction-based electro-optical modulator) to both scan the exciting beam and de-scan the emitted beam because the modulator would deviate the two beams by different amounts based on their λ.

Of even greater importance, the image captured by a CLSM in a single, 1- to 2-s scan time is commonly too noisy because the image-forming signal is simply not made up of enough photons. The image generally must be integrated electronically over several frame times to reduce the noise, just as when one is using a high-sensitivity video camera. Thus, with a CLSM, it often requires several, or many, seconds to acquire a well-resolved, high-quality fluorescence image.

If, in an attempt to reduce the number of frames that must be integrated, one tries to increase the signal reaching the PMT by raising the source brightness, by opening up the exit pinhole, or by increasing the concentration of fluorochrome, each alteration introduces new problems of its own. In fact, in CLSMs used for fluorescence imaging, if anything, one wants to reduce the light

reaching the specimen in order to avoid saturation of the fluorophores, significant bleaching, and other excitation-induced damage. There is almost an indeterminacy principle operating here: One simply cannot simultaneously achieve high temporal resolution, high spatial resolution, large pixel numbers, and a wide gray scale simultaneously. This speed limitation must be seen as a disadvantage of the CLSM.

As already discussed, two-photon confocal fluorescence microscopy (Chapter 28, *this volume*) is a promising new approach that may reduce the effect of some of these limitations in addition to providing excellent lateral and axial resolution. However, because the time between pulses is long (10–12 s) compared to the fluorescence time of organic dyes, it only produces signal 10% to 20% of the time. This low-duty cycle exacerbates the data rate limit.

While the sampling rate for obtaining whole images with the CLSM is limited, this does not imply that the temporal resolution of the detector system is inherently low. For example, one can measure relatively high-speed events with the CLSM, if one decides to sacrifice pixel numbers by reducing the size of the scanned area or even by using a single, or a few, line scan(s). In addition to the high temporal resolution, the bleaching of diffusible fluorochromes and photodynamic damage to the cell are reported to be significantly reduced when the scan is restricted to a single line (Chapter 19, *this volume*).

Another alternative for gaining speed is to use a slit instead of a pinhole for confocal scanning. This approach, although somewhat less effective than confocal imaging with small round pinholes, is surprisingly effective in suppressing the contribution of out-of-focus features. Several manufacturers have produced laser-illuminated, slit-scanning confocal microscopes that provide video-rate or direct-view imaging systems that are quite easy to operate, at a fraction of the price of the normal CLSM. However, the rapid bleaching of fluorescent dyes encountered with the slit-scanning system has been a disappointment for those hoping to gain confocal scanning speed for studies on living cells.

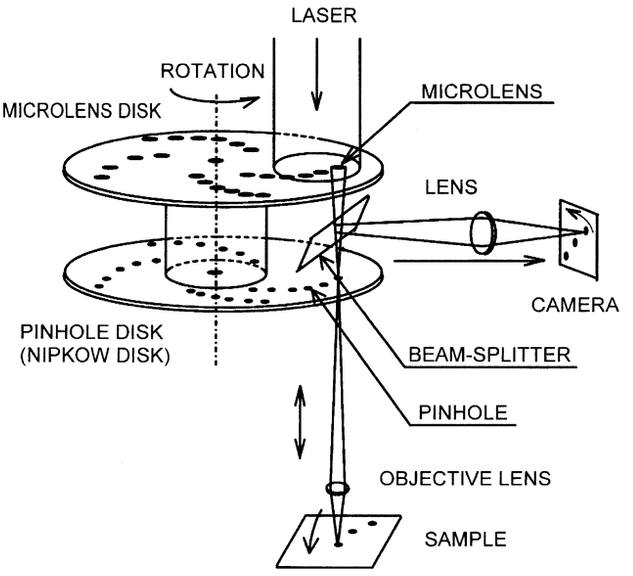

FIGURE 1.6. Schematic of optics in the CSU-10. The expanded and collimated laser beam illuminates the active portion of the upper Nipkow disk containing some 20,000 microlenses. Each microlens focuses the laser beam (through the dichromatic filter cube) onto its corresponding pinhole, thus significantly raising the fraction of the illuminating beam that is transmitted by the main Nipkow disk containing the pinhole array. From the pinholes, the beams progress down to fill the aperture of the objective lens. The objective lens generates a reduced image of the pinholes in the focal plane of the specimen.

Fluorescence given off by the illuminated points in the specimen is captured by the objective lens and focused back onto the Nipkow disk containing the pinhole array. Each pinhole now acts as its own confocal exit pinhole and eliminates fluorescence from out-of-focus regions, thus selectively transmitting fluorescence that originated from the specimen points illuminated by that particular pinhole. (However, for specimens with fluorescence distributed over large depths, some out-of-focus fluorescence can leak through adjacent pinholes in multiple pinhole systems such as the CSU-10; see text.) The rays transmitted by the exit pinholes are deflected by the dichromatic beam splitter, located between the two Nipkow disks, and proceed to the image plane. (Figure courtesy of Yokogawa Electric Corporation.)

Yokogawa Disk-Scanning Confocal System

A new confocal disk-scanning unit (CSU-10 and CSU-21) designed by Yokogawa Electric Corporation provides video-rate and faster confocal imaging with several advantages while overcoming the two major factors that had limited earlier TSM systems. The new system uses two Nipkow-type disks located one above the other with precisely aligned perforations. In place of pinholes, the first disk contains some 10,000 microlenses, each of which focuses the collimated laser beam onto a corresponding pinhole on the second disk. The microlenses increase the throughput of excitation laser from a scant 1% to 2% of conventional Nipkow disks to nearly 50%. At the same time, a dichromatic filter cube is placed between the two disks, so that light reflected or scattered from the initial disk no longer contributes unwanted background to the fluorescence signal received by the detector (Fig. 1.6). These confocal scanning units can be attached to any upright or inverted research-grade light microscope. The 1000 or so pinholes that scan the specimen in parallel at any instant of time are arranged in a unique geometrical pattern. The unique pattern reduces image streaking (found with conventional Nipkow disks) and provides uniform illumination of the whole field of view (Inoué and Inoué, 2002).

With any multiple-pinhole- (or slit-) scanning system, some light originating from outside the focal plane is transmitted through "neighboring" pinholes, so that focal discrimination is not as effective as, or the confocal stringency does not match that of, a point-scanning confocal system. Nevertheless, the Yokogawa system provides very effective focal discrimination and capability for providing striking optical sections in real time, either for direct observation through the eyepiece or captured on a video or photographic camera or a CCD. The residual out-of-focus contribution can be rapidly and effectively reduced by "unsharp masking" or "neighborhood deconvolution" digital processing. (Several examples of the dynamic cellular changes captured with the CSU-10, as well as the effectiveness of postprocessing, are illustrated in Inoué and Inoué, 2002. See also Chapter 10, *this volume*.)

In addition to the effective, real-time and faster-than-video-rate confocal fluorescence imaging in real color (which can be viewed superimposed with the brightfield or DIC image of the specimen), several observers have been impressed by the significantly slower fluorescence bleaching rate and much longer survival time for living cells observed with the CSU-10 (coupled to low-noise CCD or video cameras) compared to imaging of the same objects with point-scanning confocal systems. For example, CSU-10 imaging was found indispensable for capturing the dynamic growth, motion, and gliding of GFP-expressing microtubules in yeast cells

as well as speckle images of tubulin flux in pTk-1 tissue cells and in the thick spindles undergoing mitosis in *Xenopus* egg extracts (Waterman-Storer and Salmon, 1997; Grego *et al*., 2001; Tran *et al*., 2001; Maddox *et al*., 2002). The reasons for low-fluorescence bleaching and extended cell survival are discussed in Inoué and Inoué (2002 and in Chapter 38, *this volume*.)

The advantage of the real-time, direct-view confocal system extends beyond capturing sharp images of moving or dynamically changing objects, whose images would be blurred or distorted by the slow frame-capture rate of conventional CLSMs. For example, with a CLSM it is difficult to visualize, or even to find, minute fluorescent objects that are sparsely distributed in three dimensions. With an image intensifier CCD camera coupled to a direct-view system, the signal from such sparsely distributed objects is readily found in real time as one focuses through the specimen.

Depth of Field in Phase-Dependent Imaging

The *z*-axis resolution measured in epi-fluorescence imaging with a confocal laser scanning microscope is reported to be 1.5 µm with an NA 0.75 objective lens (Cox and Sheppard, 1993) and 0.48 µm with an NA 1.3 objective lens (Hell *et al*., 1993) at a wavelength of 514 nm. Kino reports a depth of field of 0.35 µm for NA 1.4 confocal optics, when imaging point-like reflecting objects. These numbers are in good agreement with Eqs. 2 and 3, and the height of the 3D diffraction pattern of a point object discussed earlier. In addition, Stephan Hell, as described above, has achieved even shallower field depths by superimposing two 3D diffraction spots of differing wavelengths in stimulated depletion point-scanning confocal microscopy.

How do these shallow depth of fields attainable with a confocal microscope compare with those obtainable in the absence of confocal imaging? While I could come up with no hard numbers for fluorescence microscopy without confocal imaging (except where 3D deconvolution is employed, see Chapters 23, 24, and 25, *this volume*), it is well known that the fluorescence from out-of-focus objects substantially blurs the in-focus image. On the other hand, for contrast generated by phase-dependent methods such as phase-contrast, DIC, and polarized-light microscopy, Gordon Ellis and I have obtained data that show remarkably thin optical sections in the absence of confocal imaging.

Thus, using a 100× NA 1.4 Nikon PlanApo objective lens, combined with an NA 1.35 rectified condenser whose full aperture was uniformly illuminated through a light scrambler with 546-nm light from a 100-W high-pressure Hg arc source (as described in Ellis, 1985, and in Inoué, 1986, Appendix 3), I obtained depth of fields of *ca.* 0.2, 0.25, and 0.15 µm, respectively, for phase-contrast, rectified DIC, and rectified polarized-light microscopy.

These values were obtained by examining video images of surface ridges on a tilted portion of a human buccal epithelial cell. The video signal was contrast enhanced digitally but without spatial filtration. The change in image detail that appeared with each 0.2-µm shift of focus (brought about by incrementing a calibrated stepper motor) was inspected in the image and enlarged to ~10,000× on a high-resolution video monitor. As shown in Figure 1.7, the fine ridges on the cell surface are not contiguous in the succeeding images stepped 0.2 µm apart in the polarized-light and phase-contrast images, but they are just contiguous in the DIC images. From these observations, the depth of field in the rectified polarized-light image is estimated to be somewhat below, and the DIC image just above, the 0.2-µm step height. [The phase-contrast images here should not be compared literally with the images in the two other contrast modes because the diameter of the commercially available phase annulus was rather small, and out-of-focus regions intruded obtrusively into the image. With Ellis' aperture-scanning phase-contrast microscope, the illuminating rays, and the correspondingly minute phase absorber spot, scan the outermost rim of the objective lens aperture in synchrony. Therefore, essentially the full NA of the objective lens is available to transmit the waves diffracted by the specimen. Under these conditions, the *z*-axis resolution of the optical section in phase-contrast appears to be even higher than that of the two other contrast modes shown here (Ellis, 1988; Inoué, 1994).]

For polarization microscopy of specimens with low retardances, the LC-Pol scope system devised by Oldenbourg and Mei (1995; see also Oldenbourg, 1996) also provides effective optical sectioning. The LC-Pol scope generates an image (retardance map) whose pixel brightness is proportional to the retardance of the specimen at each pixel, independent of the specimen's azimuth orientation, while the algorithm used to compute the retardance map also reduces the polarization aberrations introduced by the optics (that otherwise degrade the image; Shribak *et al*., 2002). Thus, with the LC-Pol scope system, objective lenses with NA as high as 1.4 can be used at their full aperture to detect retardances as low as 0.03 nm. The use of the high NA lenses at full aperture then provides the shallow depth of field (of less than 1-µm thickness) as illustrated in Figure 1.8. In fact, the LC-Pol scope can individually resolve two flagellar axonemes that cross each other and are separated by no more than their diameter of about 0.2 µm (Oldenbourg *et al*., 1998).

We do not yet quite understand why the depth of field of the non-confocal phase-dependent images should be so thin. It may well be that contrast generation in phase-dependent imaging involves partial coherence even at very high NAs, and that an effect similar to the one proposed elsewhere for half-wave masks (Inoué, 1989) is giving us increased lateral as well as axial resolution. Whatever the theoretical explanation turns out to be, our observations show that for phase-dependent imaging of relatively transparent objects, even in the absence of confocal optics, optical sections can be obtained (at video rate) that appear to be somewhat thinner than for fluorescence imaging in the presence of confocal optics. Moreover, they perform this function without requiring that energy be deposited in the specimen, i.e., without producing photodamage.

OTHER OPTICAL AND MECHANICAL FACTORS AFFECTING CONFOCAL MICROSCOPY

Lens Aberration

With stage- or object-scanning confocal microscopes, we saw earlier that high NA lenses with simplified design and long working distances could be used because the confocal image points (source pinhole, illuminated specimen point, and detector pinhole) all lie exactly on the optical axis of the microscope. This same principle is now used widely in the design of optical disk recorder/players.

In contrast, with TSM and CLSM sharp images of the source "pinhole(s)" must be focused over a relatively large area away from the lens axis. In addition, the objective lens and the scanner must bring images of the illuminated spot(s) and the source pinhole(s) into exact register with the exit pinhole(s), and for fluorescence microscopy, do so at different wavelengths. Thus, for these systems to function efficiently, the microscope objective lens has to be exceptionally well corrected. The field must be flat over an

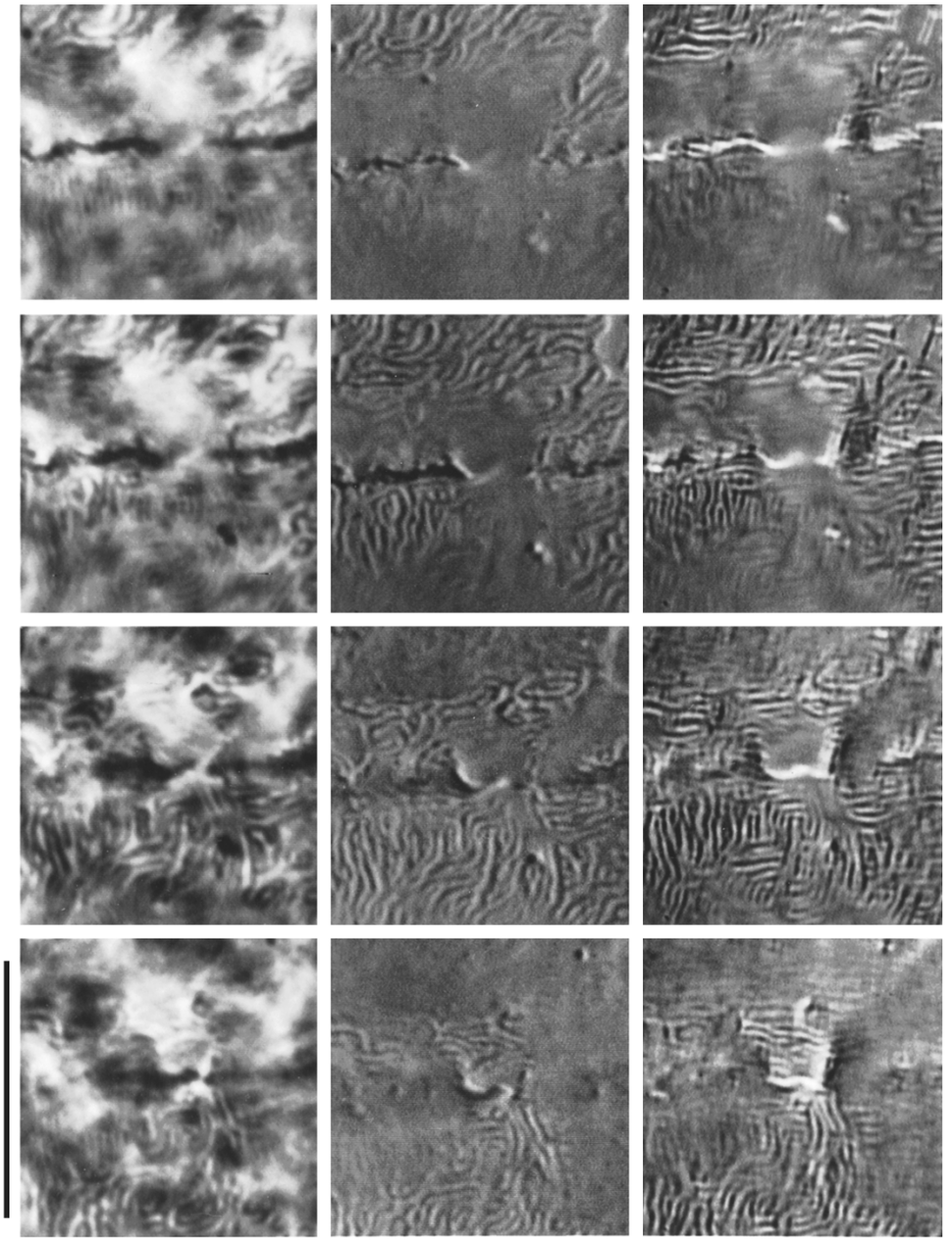

FIGURE 1.7. Optical sections of surface ridges on an oral epithelial cell. These ultrathin optical sections were obtained without confocal imaging in phase-contrast (left), rectified DIC (middle), and rectified polarized-light microscopy (right). The focus planes for the successive frames in each contrast mode were incremented 0.2 μm. Scale bar 10 μm. (See text and original article for details. From Inoué, 1988.)

appreciable area, axial and off-axis aberrations must be corrected over the field used, and lateral and longitudinal chromatic aberrations must be well corrected for both the emission *and* illuminating wavelengths. As far as is possible, the aberrations should be corrected within the objective lens without the need to use a complimentary ocular. [For details of these subjects and design of modern lenses to overcome the aberrations, see Inoué and Oldenbourg (1994), Shimizu and Takenaka (1994), and Chapter 7, *this volume*.] Finally, the lens and other optical components must have good transmission over the needed wavelength range.

These combined conditions place a strenuous requirement on the design of the objective lens. Fortunately, with the availability of modern glass stocks and high-speed computer-optimized design, a series of excellent-quality, high-NA, PlanApo, and high-UV-transmitting lenses have appeared from all four major microscope manufacturers (Leitz, Nikon, Olympus, Zeiss) during the past decade.

Even with excellent lenses, however, the image loses its sharpness when one focuses into a transparent, live, or wet specimen by more than a few micrometers from the inside surface of the coverslip. The problem here is that oil-immersion microscope objectives are designed to be used under rather stringent optical conditions, namely homogeneous immersion of everything, including the specimen itself, in a medium of $\eta = 1.52$. When such a lens is used on live or wet specimens immersed in water or physiological saline solution, even with the coverslip properly oil con-

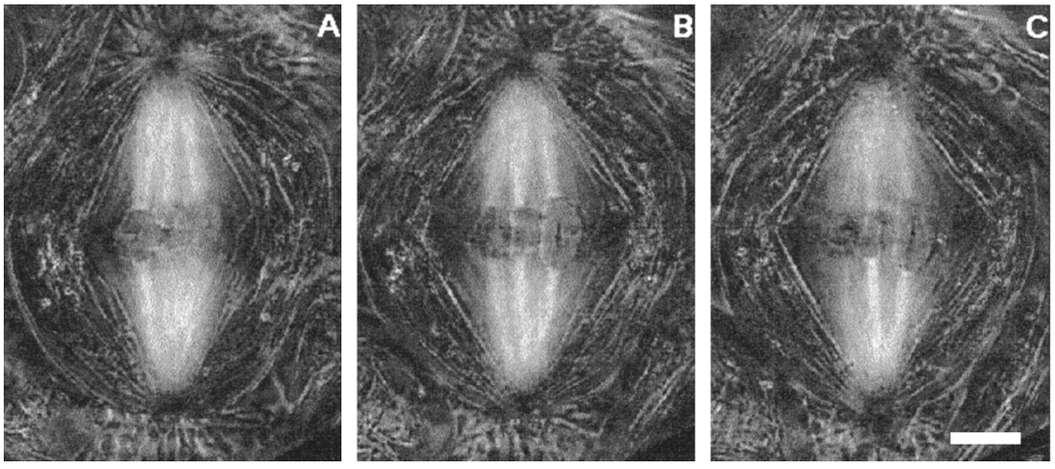

FIGURE 1.8. Optical sections of meiosis-I metaphase spindle in live spermatocyte of a crane fly *Nephrotoma sturalis* observed with the LC-Pol scope. In focus are: (A) the upper kinetochores (Ks) and their two K-fibers for the left bivalent chromosome; (B) upper Ks and fibers for the middle and right bivalents; (C) lower Ks and fibers for the middle and right bivalents. The birefringence retardation of the K-fibers, made up of a dense bundle of microtubules, is *ca.* 1 nm greater than that due to the background array of spindle microtubules. The effect of optical sectioning is more obvious in the mitochondrial threads (which are much thinner than the K-fibers and free of background birefringence) that surround the spindle. Imaged with 546-nm illumination in LC-Pol scope with Nikon 60×/1.4 NA "DIC" PlanApo objective lens combined with condenser NA at 1.0. The fine focus control was shifted 1.2 µm between (A) and (B), and 0.9 µm between (B) and (C). White = 3.0 nm retardance. Scale bar = 5 µm.

tacted to the objective lens, aberrations are no longer properly corrected once the image-forming rays traverse a significant distance in the η = 1.33 aqueous medium. Doing so distorts the unit diffraction image and alters the shape (and even the location of) the point-spread function, and does so to varying degrees as one focuses to different depths into the aqueous medium.[4] This important topic is discussed in detail in Chapters 7 and 20 (*this volume*) and in Inoué and Spring (1997, Sect. 2.5).

The same holds true also for high-NA dry objectives because they are designed under the assumption that (unless embedded in a η = 1.52 medium) the specimen lies in an infinitely thin layer placed directly against a coverslip whose thickness (generally 0.17 mm), refractive index, and dispersion conform to specification.

One approach to overcoming these problems is to switch to a water-immersion objective lens. Then the cumulative depth of the water layer between the objective lens and the focused portion of the specimen should remain unchanged with focus. Whether the objective lens is designed for homogeneous water immersion or for use in the presence of a coverslip does not matter, so long as, in the latter case, a coverslip with the proper specifications is used. In fact, however, even the small difference in η between physiological solutions, seawater, tissue, and pure water must be taken into account. While this approach does overcome some of the aberration problems, water-immersion lenses cannot be made with NAs of much above 1.25 (because of the 1.33 refractive index of water). Several manufacturers now produce high-NA water-immersion objectives with excellent correction, some with high transmissions for UV down to wavelengths of 340 nm. In our experience, the Nikon 60× 1.2 NA Plan Apochromatic, correction-collar-equipped water-immersion objective gave an impressive DIC image of diatom frustule through a 220-µm-thick layer of water between specimen and coverslip. Adjustment of the collar, as in dry- or variable-immersion objective lenses, compensates for the relative thickness of layers having higher or lower η. With the increasing use of electronic and electro-mechanical controls in confocal and conventional microscopes, it is now possible to design a superior high-NA lens with an auto-compensating correction device (possibly built outside of the objective lens) that is electronically linked to the fine focus control.

A (motor-driven) optical-correcting unit, such as the In-Focus system (Infinity Photo-Optical Company, Boulder, CO), placed in the parallel-beam region of a microscope can be used to change the focal level and/or correct for residual spherical aberration without displacing the objective lens. In fact we find that the unit can often improve the point-spread function, so that the z-axis distribution of the 3D diffraction pattern becomes more symmetric, even for "highly corrected" Plan Apochromatic objective lenses used following the manufacturer's exact specifications (see Chapters 7 and 9, *this volume*). Conversely, by appropriately linking the In-Focus drive with the objective (and condenser) lens motor drive(s), one can now substantially improve the point-spread function even when focusing deeper, for example, into a specimen residing in an aqueous medium.

Unintentional Beam Deviation

The intensity of each point in the final image from a confocal microscope is designed to measure the amount of light transmitted by the detector pinhole for the corresponding point in the specimen as it is being scanned. However, if the amount of light transmitted by the detector pinhole is modulated by factors not related to the interaction of the illuminating point of light and the specimen at that raster point, or if the confocality between the entrance pinhole, the illuminated specimen point, and the detector pinhole were to be transiently lost for any reason, one would obtain a false reading of the brightness at that point.

One such error could be introduced if a localized, lens- or prism-shaped region having a η different from that of the sur-

[4] Note also that the refractive index and dispersion of the immersion media could also be significantly affected by temperature. Some high NA immersion lenses are thus equipped with correction collars to compensate for these variations in addition to the thickness of the coverslip.

roundings were present in the path of the scanning or imaging beam. The scanning or imaging beam would then be refracted or deviated and the intensity of light reaching the detector falsely modified. Such a false signal could be difficult to distinguish from variations in a genuine signal arising from a specimen point in the focus plane. The plane of focus may also be distorted by the presence of such refracting regions (Pawley, 2002), so that one may no longer be scanning a flat optical section through the specimen (Chapter 17, *this volume*). Moreover, as discussed in the previous section, the diffraction pattern of each image point formed by an oil-immersion lens can be distorted and displaced along the *z*-axis even when a layer of optically homogeneous aqueous medium is present between the specimen and the coverslip [see Fig. 2–40 (after Gibson and Lanni, 1991) in Inoué and Spring, 1997]. Attempts to correct some beam deviations by interferometric measurements of the specimen have been published (Kam *et al*., 2001).

Clearly, vibration of the microscope, and even minor distortions of the mechanical components that support the optics or the specimen, may introduce misalignment between the two pinholes and what was supposed to be the confocal point in the specimen. This could lead to short-term periodic errors or longer-term drift. Antivibration tables that isolate the instrument from building and floor vibrations are commonly used to support confocal microscopes. While such a support is useful and may be essential in some building locations, it does not eliminate the influence of airborne vibration, which can in fact raise major havoc in microscopy (G.W. Ellis, personal communication, 1966). Nor does it eliminate the influence of thermal drift or vibration arising from the operation of the instrument.

Given the need to precisely maintain the confocal alignment and to use some form of mechano-optical scanning within the instrument, a confocal microscope is especially susceptible to vibration and problems of mechanical distortion. Indeed, once the complex optical, electro-optical, mechanical, and electronic systems have been appropriately designed, the success of one confocal instrument over another may well depend on its immunity to vibration, in addition to the friendliness of its user interface. Yokogawa's disk-scanning system, while with somewhat reduced confocal stringency, turns out to be remarkably immune to vibration problems.

CONTRAST TRANSFER AND RESOLUTION IN CONFOCAL VERSUS NON-CONFOCAL MICROSCOPY

In addition to designing and successfully demonstrating the power of stage-scanning confocal microscopy, Wilson and colleagues have extensively analyzed the theoretical foundations of confocal microscope imaging (see Wilson and Sheppard, 1984; Wilson, 1990; Chapters 11, 22, and 23, *this volume*). Their mathematical treatment leads to the somewhat surprising conclusion that the ultimate limit of resolution (i.e., the cut-off spatial frequency or spacing at which image contrast of periodic objects drops to zero) obtainable with *coherent confocal* microscopy is identical with that for *incoherent non-confocal* microscopy. However, compared to incoherent non-confocal optics, image contrast should rise much more sharply with coherent confocal optics as the spatial period is increased. Therefore, the practical resolution attained at threshold contrast (i.e., the minimum contrast required for the spacing to be detected) was expected to be significantly greater with confocal optics than with conventional non-confocal optics.

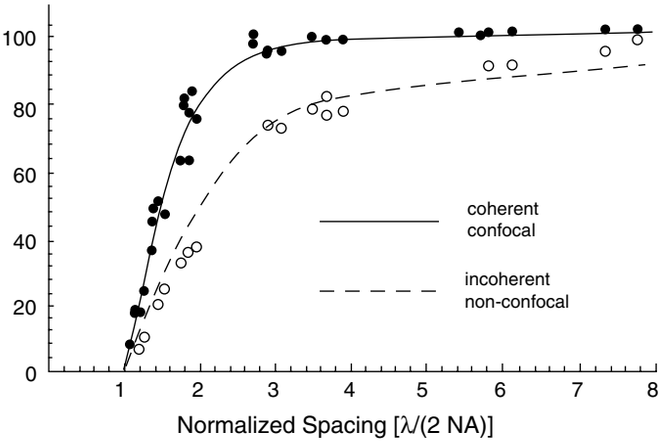

FIGURE 1.9. Experimental contrast transfer values measured as a function of the spatial period of line gratings using a laser beam-scanning microscope in the confocal reflection mode (solid points) and in the non-confocal transmission mode (circles). In both imaging modes, PlanApo objective lenses (Nikon Inc., Melville, NY) with numerical apertures (NAs) ranging from 0.45 to 1.4 and laser wavelengths (λ) of 514.5 nm or 488 nm were used. Spatial periods are expressed in units of the limiting wavelength, λ/2(NA), to normalize the data taken with different laser λ and lenses of different NA. We call data presented in this fashion the contrast transfer characteristic (CTC).

Continuous lines are theoretical curves displaying calculated CTCs for the coherent confocal and the incoherent non-confocal imaging modes. Comparison of the two CTC curves shows that, while the limiting resolutions are identical for both imaging modes, the contrast due to fine detail in the specimen is maintained much better with confocal optics. (The microscope was a prototype built by Hamamatsu Photonics Kabushiki Kaisha, Japan. It was used with the detector pinhole diameter reduced to a small fraction of the Airy disk diameter. From Oldenbourg *et al*., 1993.)

We have confirmed these predictions by direct measurement on test gratings that we fabricated by electron lithography with spacings down to 0.1 µm. Indeed, with confocal optics equipped with a small exit pinhole, the contrast transfer efficiency rose to 80% at twice (and reached 100% at three times) the cut-off spacing. With incoherent non-confocal imaging, 80% contrast transfer was not attained until four times and did not even reach the 100% transfer rate at eight times the cut-off spacing (Fig. 1.9)!

SUMMARY

- The limiting resolution of all microscopes depends on the λ of the light used and the NA of the objective and condenser lenses. Dirty or misaligned optics or vibration, or both, can reduce the achieved resolution. Test resolution regularly, and especially pay attention to the iris setting and full illumination of the condenser aperture, to assure optimal performance.
- A small detector pinhole in the confocal microscope is essential if the maximum optical sectioning capability and resolution of the instrument are to be realized concurrently. Correct alignment and use of this control is very important. However, a larger pinhole may be required to improve the signal when there is limited light level, motion in the specimen, or fading of fluorescence.
- By opening the confocal exit pinhole (to not much greater than the Airy disk diameter), one loses the advantage of higher X–Y resolution in fluorescence microscopy but retains much of the capability for rejecting out-of-focus information while also gaining in the fluorescence signal.

- The ultimate resolution limit of a CLSM in the reflection mode is the same as that of a conventional light microscope, but the contrast that it produces from features is higher. For fluorescence imaging, the resolution in a confocal microscope can be $\sim\sqrt{2}$ greater than with conventional microscopy, but only *if* the confocal detector pinhole is appreciably smaller than the Airy disk produced by a point fluorescent object.
- CLSM is not a cure-all for all biological studies. Its sampling speed is limited, and it does not lend itself to using either interference effects to produce contrast, such as phase or DIC, which have been found to be relatively innocuous to living cells, or polarization contrast that can reveal fine structural dynamics noninvasively.
- Video microscopy can take advantage of the various types of interference and polarizing contrast not easily implemented in the CLSM. Therefore, it is ideal for dynamic, high-resolution observations of living specimens and for tracking the behavior of macromolecular assemblies.
- Holographic microscopy is a field with intriguing promise that is so far beset by practical difficulties.
- Two-photon microscopy and CLSMs provide high-confocal stringency and, in general, are methods of choice for obtaining clear, high-resolution optical sections of the fluorescence distribution in 3D fluorescent specimens. However, for capturing well-resolved optical sections of highly dynamic specimens, or for detection of sparsely distributed minute fluorescent objects, the newer disk-scanning confocal systems employing microlenses on the pinholes may well be the system of choice.

ACKNOWLEDGMENT

This chapter is an updated version of the chapter in the first and second editions. We thank the staff of Yokogawa Electric Corporation for Figure 1.6 and Drs. James LaFountain and Rudolf Oldenbourg for making available the yet unpublished source material for Figure 1.8. We are most grateful to Professor Yoshinori Fujiyoshi of Kyoto University, whose support made the preparation of this chapter possible.

REFERENCES

Abbe, E., 1873, Beiträge zur Theorie des Mikroskops und der mikroskopischen Wahrnehmung, *Schultzes Arc. f. Mikr. Anat.* 9:413–468.

Abbe, E., 1884, Note on the proper definition of the amplifying power of a lens or a lens-system, *J. Royal Microsc. Soc.* 4:348–351.

Agard, D.A., and Sedat, J.W., 1983, Three dimensional architecture of a polytene nucleus, *Nature* 302:676–681.

Agard, D.A., Hiraoka, Y., Shaw, P., and Sedat, J.W., 1989, Fluorescence microscopy in three dimensions, *Methods Cell Biol.* 30: 353–377.

Allen, R.D., 1985, New observations on cell architecture and dynamics by video-enhanced contrast optical microscopy, *Annu. Rev. Biophys. Biophysical Chem.* 14:265–290.

Allen, R.D., Travis, J.L., Allen, N.S., and Yilmaz, H., 1981a, Video-enhanced contrast polarization (AVEC-POL) microscopy: A new method applied to the detection of birefringence in the motile reticulopodial network of *Allogromia laticollaris*, *Cell Motil.* 1:275–289.

Allen, R.D., Allen, N.S., and Travis, J.L., 1981b, Video-enhanced contrast, differential interference contrast (AVEC-DIC) microscopy: A new method capable of analyzing microtubule-related motility in the reticulopodial network of *Allogromia laticollaris*, *Cell Motil.* 1:291–302.

Amos, W.B., White, J.G., and Fordham, M., 1987, Use of confocal imaging in the study of biological structures, *Appl. Opt.* 26:3239–3243.

Åslund, N., Carlsson, K., Liljeborg, A., and Majlof, L., 1983, PHOIBOS, a microscope scanner designed for micro-fluorometric applications, using laser induced fluorescence. In: *Proceedings of the Third Scandinavian Conference on Image Analysis, Studentliteratur*, Lund, p. 338.

Åslund, N., Liljeborg, A., Forsgren, P.-O., and Wahlsten, S., 1987, Three dimensional digital microscopy using the PHOIBOS scanner, *Scanning* 9:227–235.

Baxes, G.A., 1984, *Digital Image Processing: A Practical Primer*, Prentice-Hall, Englewood Cliffs, New Jersey.

Berek, M., 1927, Grundlagen der Tiefenwahrnehmung im Mikroskop, *Marburg Sitzungs Ber.* 62:189–223.

Born, M., and Wolf, E., 1980, *Principles of Optics*, 6th ed., Pergamon Press, Oxford, England.

Boyde, A., 1985a, Tandem scanning reflected light microscopy (TSRLM), Part 2: Pre-MICRO 84 applications at UCL, *Proc. Royal Microsc. Soc.* 20:131–139.

Boyde, A., 1985b, Stereoscopic images in confocal (tandem scanning) microscopy, *Science* 230:1270–1272.

Boyde, A., 1987, Colour-coded stereo images from the tandem scanning reflected light microscope (TSRLM), *J. Microsc.* 146:137–142.

Brakenhoff, G.J., Blom, P., and Barends, P., 1979, Confocal scanning light microscopy with high aperture immersion lenses, *J. Microsc.* 117:219–232.

Brakenhoff, G.J., van der Voort, H.T.M., van Spronsen, E.A., Linnemans, W.A.M., and Nanninga, N., 1985, Three dimensional chromatin distribution in neuroblastoma nuclei shown by confocal scanning laser microscopy, *Nature* 317:748–749.

Brakenhoff, G.J., van der Voort, H.T.M., van Spronsen, E.A., and Nanninga, N., 1986, Three dimensional imaging by confocal scanning fluorescence microscopy. In: *Recent Advances in Electron and Light Optical Imaging in Biology and Medicine*, Vol. 483 (A. Somlyo, ed.), Ann. N.Y. Acad. Sci., New York, pp. 405–414.

Brakenhoff, G.J., van Spronsen, E.A., van der Voort, H.T.M., and Nanninga, N., 1989, Three dimensional confocal fluorescence microscopy, *Methods Cell Biol.* 30:379–398.

Bright, G.R., Fisher, G.W., Rogowska, J., and Taylor, D.L., 1989, Fluorescence ratio imaging microscopy, *Methods Cell Biol.* 30:157–192.

Cagnet M., Françon, M., and Thrierr, J.C., 1962, *Atlas of Optical Phenomena*, Springer-Verlag, Berlin.

Carlsson, K., Danielsson, P., Lenz, R., Liljeborg, A., Majlof, L., and Åslund, N., 1985, Three-dimensional microscopy using a confocal laser scanning microscope, *Opt. Lett.* 10:53–55.

Castleman, K.R., 1979, *Digital Image Processing*, Prentice-Hall, Englewood Cliffs, New Jersey.

Castleman, K.R., 1987, Spatial and photometric resolution and calibration requirements for cell image analysis instruments, *Appl. Opt.* 26:3338–3342.

Castleman, K.R., 1993, Resolution and sampling requirements for digital image processing, analysis, and display. In: *Electronic Light Microscopy* (D. Shotton, ed.), Wiley-Liss Inc., New York, pp. 71–94.

Conchello, J.-A., Heym, J.P., Wei, J.L., and Lichtman, J.W., 1997, NOVEL reflected light confocal profilometer, *Proc. SPIE Conf.* 2984:101–112.

Cox, G., and Sheppard, C., 1993, Effects of image deconvolution on optical sectioning in conventional and confocal microscopes, *Bioimaging* 1:82–95.

Cox, I.J., and Sheppard, C.J.R., 1983, Scanning optical microscope incorporating a digital framestore and microcomputer, *Appl. Opt.* 22:1474–1478.

Cox, I.J., and Sheppard, C.J.R., 1986, Information capacity and resolution in an optical system, *J. Opt. Soc. Am.* 3:1152–1158.

Cremer, C., and Cremer, T. 1978, Considerations on a laser-scanning-microscope with high resolution and depth of field, *Microsc. Acta* 81:31–44.

Davidovits, P., and Egger, M.D., 1971, Scanning laser microscope for biological investigations, *Appl. Opt.* 10:1615–1619.

Davidovits, P., and Egger, M.D., 1972, U.S. Patent #3,643,015, Scanning Optical Microscope.

Denk, W., and Webb, W.W., 1987, Displacement fluctuation spectroscopy of the sensory hair bundles of mechanosensitive cells of the inner ear, *Bull. Am. Phys. Soc.* 32:645.

Denk, W., Strickler, J.H., and Webb, W.W., 1990, Two-photon laser scanning fluorescence microscopy, *Science* 248:73–76.

Egger, M.D., 1989, The development of confocal microscopy, *Trends Neurosci.* 12:11.

Egger, M.D., and Petráň, M., 1967, New reflected-light microscope for viewing unstained brain and ganglion cells, *Science* 157:305–307.

Ellis, G.W., 1966, Holomicrography: Transformation of image during reconstruction a posteriori, *Science* 154:1195–1196.

Ellis, G.W., 1978, Advances in visualization of mitosis *in vivo*. In: *Cell Reproduction, in Honor of Daniel Mazia* (E. Dirksen, D. Prescott, and C.F. Fox, eds.), Academic Press, New York, pp. 465–476.

Ellis, G.W., 1979, A fiber-optic phase-randomizer for microscope illumination by laser, *J. Cell Biol.* 83:303a.

Ellis, G.W., 1985, Microscope illuminator with fiber-optic source integrator, *J. Cell Biol.* 101:83a.

Ellis, G.W., 1988, Scanned aperture light microscopy In: *Proceedings of the Forty-sixth Annual Meeting of EMSA*, San Francisco Press, San Francisco, pp. 48–49.

Fay, F.S., Fogarty, K.E., and Coggins, J.M., 1985, Analysis of molecular distribution in single cells using a digital imaging microscope. In: *Optical Methods in Cell Physiology* (P. De Weer and B.M. Salzberg, eds.), John Wiley & Sons, New York.

Flory, L.E., 1951, The television microscope, *Cold Spring Harbor Symp. Quant. Biol.* 16:505–509.

Freed, J.J., and Engle, J.L. 1962, Development of the vibrating-mirror flying spot microscope for ultraviolet spectrophotometry, *Ann. N.Y. Acad. Sci.* 97:412–448.

Fuchs, H., Pizer, S.M., Heinz, E.R., Bloomberg, S.H., Tsai, L-C., and Strickland, D.C., 1982, Design and image editing with a space-filling 3D display based on a standard raster graphics system, *Proc. Soc. Photo. Opt. Instrum. Eng.* 367:117–127.

Gibson, S.F., and Lanni, F., 1991. Experimental test of an analytical model of aberration in an oil-immersion objective lens used in three-dimensional light microscopy, *J. Opt. Soc. Am.* A 8:1601–1613.

Goldstein, S.R., Hubin, T., Rosenthal, S., and Washburn, C., 1990, The VRIDICOM: a video rate image dissector confocal microscope. In: *Optical Microscopy for Biology* (B. Herman and K. Jacobson, eds.), Wiley-Liss, Inc., New York, pp. 59–72.

Gonzales, R.C., and Wintz, P., 1987, *Digital Image Processing*, 2nd ed., Addison-Wesley, Reading, Massachusetts.

Grego, S., Cantillana, V., and Salmon, E.D., 2001, Microtubule treadmilling in vitro investigated by fluorescence speckle and confocal microscopy, *Biophys. J.* 81:66–78.

Gustafsson, M.G.L., 2000, Surpassing the lateral resolution limit by a factor of two using structured illumination microscopy, *J. Microsc.* 198:82–87.

Hamilton, D.K., and Wilson, T. 1984, Two-dimensional phase imaging in the scanning optical microscope, *Appl. Opt.* 23:348–352.

Hansen, E.W., 1986, Appendix II. In: *Video Microscopy* (S. Inoué, ed.), Plenum Press, New York, pp. 467–475.

Hard, R., Zeh, R., and Allen, R.D., 1977, Phase-randomized laser illumination for microscopy, *J. Cell Sci.* 23:335–343.

Harris, J.L., 1964, Diffraction and resolving power, *J. Opt. Soc. Am.* 54:931–936.

Hecht, E., 1987, *Optics*, 2nd ed., Addison-Wesley, Reading, Massachusetts.

Hell, S.W., and Wichmann, J., 1994, Breaking the diffraction resolution limit by stimulated emission: stimulated-emission-depletion fluorescence microscopy, *Opt. Lett.* 19:780–782.

Hell, S.W., Reiner, G., Cremer, C., and Stelzer, E.H.K., 1993, Aberrations in confocal fluorescence microscopy induced by mismatches in refractive index, *J. Microsc.* 169:391–405.

Hellwarth, R., and Christensen, P., 1974, Nonlinear optical microscopic examination of structure in polycrystalline ZnSe, *Optics Comm.* 12:318–322.

Hoffman, R., and Gross, L., 1975, Modulation contrast microscopy, *Appl. Opt.* 14:1169–1176.

Hopkins, H.H., 1951, The concept of partial coherence in optics, *Proc. Royal Soc. Lond.* 208A:263.

Hopkins, H.H., and Barham, P.M., 1950, The influence of the condenser on microscopic resolution, *Proc. Royal Soc. Lond.* 63B:737–744.

Ichihara, A., Tanaami, T., Isozaki, K., Sugiyama, Y., Kosugi, Y., Mikuriya, K., Abe, M., and Uemura, I., 1996, High-speed confocal fluorescence microscopy using a Nipkow scanner with microlenses — for 3-D imaging of single fluorescent molecule in real-time, *Bioimages* 4:57–62.

Ingelstam, E., 1956, Different forms of optical information and some interrelations between them. In: *Problem in Contemporary Optics*, Istituto Nazionale di Ottica, Arcetri-Firenze, pp. 128–143.

Inoué, S., 1981, Video image processing greatly enhances contrast, quality, and speed in polarization based microscopy, *J. Cell Biol.* 89:346–356.

Inoué, S., 1986, *Video Microscopy*, Plenum Press, New York.

Inoué, S., 1988, Progress in video microscopy, *Cell Motil. Cytoskel.* 10:13–17.

Inoué S., 1989, Imaging of unresolved objects, superresolution, and precision of distance measurement, with video microscopy, *Methods Cell Biol.* 30:85–112.

Inoué S., 1994, Ultra-thin optical sectioning and dynamic volume investigation with conventional light microscopy. In: *Three-Dimensional Confocal Microscopy* (J.K. Stevens, L.R. Mills, and J. Trogadis, eds.), Academic Press, San Diego, pp. 397–419.

Inoué, S., and Inoué, T.D., 1986, Computer-aided stereoscopic video reconstruction and serial display from high-resolution light-microscope optical sections. In: *Recent Advances in Electron and Light Optical Imaging in Biology and Medicine*, Vol. 483 (A. Somlyo, ed.), Ann. N.Y. Acad. Sci., New York, pp. 392–404.

Inoué, S., and Inoué, T.D., 2002, Direct-view high-speed confocal scanner — the CSU-10. In: *Cell Biological Applications of Confocal Microscopy*, 2nd ed. (B. Matsumoto, ed.), Academic Press, San Diego, pp. 87–123.

Inoué, S., and Oldenbourg, R., 1995, Optical instruments: Microscopes. In: *Handbook of Optics*, 2nd ed., Vol. 2 (M. Bass, ed.), McGraw-Hill, New York, pp. 17.1–17.52.

Inoué, S., and Spring, K., 1997, *Video Microscopy*, 2nd ed., Plenum Press, New York.

Inoué, S., Goda, M., and Knudson, R.A., 2001a, Centrifuge polarizing microscope. II. Sample biological applications, *J. Microsc.* 201:357–367.

Inoué, S., Knudson, R.A., Goda, M., Suzuki, K., Nagano, C., Okada, N., Takahashi, H., Ichie, K., Iida, M., and Yamanaka, K., 2001b, Centrifuge polarizing microscope. I. Rationale, design, and instrument performance, *J. Microsc.* 201:341–356.

Inoué, S., Shimomura, O., Goda, M., Shribak, M., and Tran, P.T., 2002, Fluorescence polarization of green fluorescent protein (GFP), *Proc. Natl. Acad. Sci.* 99:4272–4277.

Kam, Z., Hanser, B., Gustafsson, M.G.L., Agard, D.A., and Sedat, J.W., 2001, Computational adaptive optics for live three-dimensional biological imaging, *Proc. Natl. Acad. Sci.* 98:3790–3795.

Klar, T.A., Jacobs, S., Dyba, M., Egner, A., and Hell, S.W., 2000, Fluorescence microscopy with diffraction resolution barrier broken by stimulated emission, *Proc. Natl. Acad. Sci.* 97:8206–8210.

Koester, C.J., 1980, Scanning mirror microscope with optical sectioning characteristics: Applications in ophthalmology, *Appl. Opt.* 19:1749–1757.

Kubota, H., and Inoué, S., 1959, Diffraction images in the polarizing microscope, *J. Opt. Soc. Am.* 49:191–198.

Leith, E.N., and Upatnieks, J., 1963, Wavefront reconstruction with continuous-tone objects, *J. Opt. Soc. Am.* 53:1377–1381.

Leith, E.N., and Upatnieks, J., 1964, Wavefront reconstruction with diffused illumination and 3D objects, *J. Opt. Soc. Am.* 54:1295–1301.

Lewin, R., 1985, New horizons for light microscopy, *Science* 230:1258–1262.

Linfoot, E.H., and Wolf, E., 1953, Diffraction images in systems with an annular aperture, *Proc. Phys. Soc. B* 66:145–149.

Linfoot, E.H., and Wolf, E., 1956, Phase distribution near focus in an aberration-free diffraction image, *Proc. Phys. Soc. B* 69:823–832.

Maddox, P., Desai, A., Oegema, K., Mitchison, T.J., and Salmon, E.D., 2002, Poleward microtubule flux is a major component of spindle dynamics and anaphase A in mitotic *Drosophila* embryos, *Curr. Biol.* 12:1670–1674.

McCarthy, J.J., and Walker, J.S., 1988, Scanning confocal optical microscopy, *EMSA Bull.* 18:75–79.

Minsky, M., 1957, U.S. Patent #3013467, Microscopy Apparatus.

Minsky, M., 1988, Memoir on inventing the confocal scanning microscope, *Scanning* 10:128–138.

Montgomery, P.O., Roberts, F., and Bonner, W., 1956, The flying-spot monochromatic ultra-violet television microscope, *Nature* 177:1172.

Nipkow, P., 1884, German Patent #30,105.

Nomarski, G., 1955, Microinterférométre différentiel à ondes polarisées, *J. Phys. Radium* 16:S9–S13.

Oldenbourg, R., 1996, A new view on polarization microscopy, *Nature* 381:811–812.

Oldenbourg, R., and Mei, G., 1995, New polarized light microscope with precision universal compensator, *J. Microsc.* 180:140–147.

Oldenbourg, R., Salmon, E.D., and Tran, P.T., 1998, Birefringence of single and bundled microtubules, *Biophys. J.* 74:645–654.

Oldenbourg, R., Terada, H., Tiberio, R., and Inoué, S., 1993, Image sharpness and contrast transfer in coherent confocal microscopy, *J. Microsc.* 172:31–39.

Pawley, J.B., 2002, Limitations on optical sectioning in live-cell confocal microscopy, *Scanning* 21:241–246.

Petráň, M., Hadravsky, M., Egger, D., and Galambos, R., 1968, Tandem-scanning reflected-light microscope, *J. Opt. Soc. Am.* 58:661–664.

Quate, C.F., 1980, Microwaves, acoustic and scanning microscopy. In: *Scanned Image Microscopy* (E.A. Ash, ed.), Academic Press, San Diego, pp. 23–55.

Sharnoff, M., Brehm, L., and Henry, R., 1986, Dynamic structures through microdifferential holography, *Biophys. J.* 49:281–291.

Sheppard, C.J.R., and Choudhury, A., 1977, Image formation in the scanning microscope, *Optica* 24:1051.

Sheppard, C.J.R., Gannaway, J.N., Walsh, D., and Wilson, T., 1978, *Scanning Optical Microscope for the Inspection of Electronic Devices*, Microcircuit Engineering Conference, Cambridge.

Sher, L.D., and Barry, C.D., 1985, The use of an oscillating mirror for 3D displays. In: *New Methodologies in Studies of Protein Configuration* (T.T. Wu, ed.), Van Nostrand-Reinhold, Princeton, New Jersey.

Shimizu, Y., and Takenaka, H., 1994, Microscope objective design. In: *Advances in Optical and Electron Microscopy*, Vol. 14 (C. Sheppard and T. Mulvey, eds.), Academic Press, San Diego, pp. 249–334.

Shotten, D., ed., 1993, *Electronic Light Microscopy: The Principles and Practice of Video-enhanced Contrast, Digital Intensified Fluorescence, and Confocal Scanning Light Microscopy*, John Wiley & Sons, New York.

Shribak, M., Inoué, S., and Oldenbourg, R., 2002, Polarization aberrations caused by differential transmission and phase shift in high-numerical-aperture lenses: theory, measurement, and rectification, *Opt. Eng.* 41:943–954.

Smith, L.W., and Osterberg, H., 1961, Diffraction images of circular self-radiant disks, *J. Opt. Soc. Am.* 51:412–414.

Squirrel, J.M., Wokosin, D.L., White, J.G., and Bavister, B.D., 1999, Long-term two-photon fluorescence imaging of mammalian embryos without compromising viability, *Nature Biotech.* 17:763–767.

Stevens, J.K., Mills, L.R., and Trogadis, J., 1994, *Three-Dimensional Confocal Microscopy*, Academic Press, San Diego.

Streibl, N., 1985, Three dimensional imaging by a microscope, *J. Opt. Soc. Am.* A 2:121–127.

Suzuki, T., and Hirokawa, Y., 1986, Development of a real-time scanning laser microscope for biological use, *Appl. Opt.* 25:4115–4121.

Tanasugarn, L., McNeil, P., Reynolds, G.T., and Taylor, D.L., 1984, Microspectrofluorometry by digital image processing: Measurement of cytoplasmic pH, *J. Cell Biol.* 89:717–724.

Tolardo di Francia, G., 1955, Resolving power and information, *J. Opt. Soc. Am.* 45:497–501.

Tran, P.T., Marsh, L., Doye, V., Inoué, S., and Chang, F., 2001, A mechanism for nuclear positioning in fission yeast based on microtubule pushing, *J. Cell Biol.* 153:397–411.

Tsien, R.Y., 1989, Fluorescent indicators of ion concentration, *Methods Cell Biol.* 30:127–156.

Volkmer, A., Cheng, J.-X., and Xie, X. S., 2001, Vibrational imaging with high sensitivity via epidetected coherent anti-Stokes Raman scattering microscopy, *Phys. Rev. Lett.* 87:023901-1–023901-4.

Waterman-Storer, C.M., and Salmon, E.D., 1997, Actomyosin-based retrograde flow of microtubules in the lamella of migrating epithelial cells influences microtubule dynamic instability and turnover and is associated with microtubule breakage and treadmilling, *J. Cell Biol.* 139:417–434.

White, J.G., Amos, W.B., and Fordham, M., 1987, An evaluation of confocal versus conventional imaging of biological structures by fluorescence light microscopy, *J. Cell Biol.* 105:41–48.

Wijnaendts van Resandt, R.W., Marsman, H.J.B., Kaplan, R., Davoust, J., Stelzer, E.H.K., and Strickler, R., 1985, Optical fluorescence microscopy in three dimensions: Microtomoscopy, *J. Microsc.* 138:29–34.

Wilke, V., Gödecke, U., and Seidel, P., 1983, Laser-scan-mikroskop, *Laser and Optoelecktron* 15:93–101.

Wilson, T., 1985, Scanning optical microscopy, *Scanning* 7:79–87.

Wilson, T., 1990, *Confocal Microscopy*, Academic Press, London.

Wilson, T., and Sheppard, C., 1984, *Theory and Practice of Scanning Optical Microscopy*, Academic Press, London.

Wilson, T., Gannaway, J.N., and Johnson, P., 1980, A scanning optical microscope for the inspection of semiconductor materials and devices, *J. Microsc.* 118:390–314.

Xiao, G.Q., and Kino, G.S., 1987, A real-time confocal scanning optical microscope. In: *Proceedings of SPIE*, Vol. 809, *Scanning Imaging Technology* (T. Wilson and L. Balk, eds.), pp. 107–113.

Young, J.Z., and Roberts, F., 1951, A flying-spot microscope, *Nature* 167: 231.

Zernicke, V.F., 1935, Das Phasenkontrastverfahren bei der mikroskopischen Beobachtung, *Z. Tech. Phys.* 16:454–457.

Zworykin, V.K., 1934, The iconoscope — a modern version of the electric eye, *Proceedings of IRE* 22:16–32.

Zworykin, V.K., and Morton, G.A., 1954, *Television: The Electronics of Image Transmission in Color and Monochrome*, 2nd ed., John Wiley & Sons, New York.